Analysis, Classification, and Design of Tendon-Driven Mechanisms

Ryuta Ozawa, *Member, IEEE*, Hiroaki Kobayashi, *Member, IEEE*, and Kazunori Hashirii

***Abstract*—This paper analyzes tendon-driven mechanisms (TDMs) with active and passive tendons and proposes a method for designing TDMs. First, we group TDMs into six classes according to their controllability and the number of driving degrees of freedom. In this classification system, the conventional underactuated mechanisms are grouped into three classes, two of which have often previously been grouped together although they have different manipulation abilities. Next, we analyze bias forces to separate and decouple a given TDM into several smaller TDMs. Finally, we propose a design method for combining smaller TDMs into an appropriate TDM. Using this method, we can easily determine an appropriate tendon transmission that meets the requirements for the number of tendons, the hardware of the tendon routing, and arbitrary joint constraint that has useful applications in prosthetic and biomimetic hands. Numerical examples show that the proposed method guarantees a nonsingular series actuation transmission and that the designed underactuated TDMs could achieve arbitrary stiffness independent of the actuation effort compared with the conventional underactuated TDM with torsion springs.**

***Index Terms*—Cable-driven mechanisms, tendon-driven mechanisms (TDMs), transmission design, underactuated mechanisms, wire-driven mechanisms.**

I. Introduction

ROBOTIC manipulators typically execute complex tasks using their joints, which are independently controlled by actuators. Recently, underactuated robotic mechanisms have been developed for robotic and prosthetic hands to reduce the number of actuators, which are one of the heaviest components of robotic systems [1], [2]. These underactuated mechanisms are useful for adaptive grasping, in which several joints move in conjunction to grasp an object using simple control methods [3]. This type of adaptive gripper has many practical applications, such as grasping large objects in a space station [4], [5], grasping fast-moving objects [6], and grasping an object with either a palm or fingertips using prosthetic hands [1]. Underactuated mechanisms are also useful in the development of biomimetic robotic fingers that have the ability to flex their proximal interphalangeal (PIP) and distal interphalangeal (DIP) joints in the same manner as human fingers [4], [7]. These underactuated mechanisms have been developed with either a parallel linkage or tendon-driven mechanisms (TDMs), using both actuators and passive springs.

Parallel linkage mechanisms with minimal actuation have been widely used to develop underactuated planar mechanisms and have been analyzed to optimize their isotropic torque distribution and grasping stability [8]. Generally, parallel linkage mechanisms are limited to planar cases and are combined with other drive systems to move in space [9] except [10]. Furthermore, TDMs have been used to develop a lightweight spatial arm [11], [12], robotic hands [13], [14], a suspended high-speed system [15], and a humanoid robot [16]. This paper is focused on TDMs using active and passive tendons that are passed over joints using pulleys and sheaths. Pulleys are used to transmit the driving force to a series of joints. Designs using wire-routing over pulleys suffer from an increased mechanical complexity. On the other hand, sheaths are used to simplify the wire routing and skip some joints by transmitting the driving force only to the terminal joints. However, the sheaths generally introduce a large friction force that degrades the control response [17].

The tensile force of the tendons generates only unilateral traction, and each tendon is coupled to several joints. Therefore, the analysis of TDMs is generally more complex than that of conventional drive systems that generate a bilateral driving force. TDMs have been analyzed by investigating their transmission efficiency under various parameters of the elasticity and friction of the tendons [11] and by determining the optimal isotropic transmission performances of an end-point force that optimizes the condition number of the tendon Jacobian that was fixed in a pseudo-triangular form [18]. The kinematic structures of TDMs were analyzed by determining the equivalent structure of the tendon Jacobian, which corresponds to the change of the tendon's order [19] and the redundancy and controllability of the TDM [20]. These studies assumed that each tendon is driven by independent actuators; however, these authors did not analyze underactuated TDMs and did not propose a method to design the structure of the tendon Jacobian.

In this paper, we propose a design method for TDMs with active and passive tendons based on kinematic analyses. First, we classify the TDMs into several groups and discuss their differences, which have not previously been described for conventional TDMs. Moreover, we investigate the separability of a given TDM according to its bias force independence. Based on this separability, we propose a design method for TDMs. This method enables us to efficiently design joint constraint

Manuscript received April 27, 2012; revised January 30, 2013 and July 17, 2013; accepted October 14, 2013. Date of publication November 13, 2013; date of current version April 1, 2014. This paper was recommended for publication by Associate Editor L. Villani and Editor B. J. Nelson upon evaluation of the reviewers' comments.

R. Ozawa is with the Department of Robotics, Ritsumeikan University, Kyoto 603-8577, Japan (e-mail: ryuta@se.ritsumei.ac.jp).

H. Kobayashi is with the Department of Mechanical Engineering Informatics, Meiji University, Kawasaki 214-8571, Japan (e-mail: kobayasi@isc.meiji.ac.jp).

K. Hashirii is with Nabel Co., Ltd., Kyoto 601-8444, Japan (e-mail: k.hashirii@gmail.com).

Color versions of one or more of the figures in this paper are available online at http://ieeexplore.ieee.org.

Digital Object Identifier 10.1109/TRO.2013.2287976

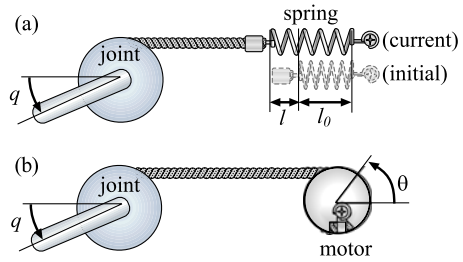

Fig. 1. Tendons. (a) Passive tendon connected with a spring. (b) Active tendon driven by an actuator.

motions for underactuated robots and fully actuated robots. In this design, a TDM is constructed from a combination of subtendon Jacobian structures, which have not been considered in a force optimization problem in a fixed tendon Jacobian [18]. The proposed method and the force optimization problem complement each other. The proposed method can be applied to spatial manipulators with multiple driving degree of freedom (DOF) and can be easily expanded to TDMs combined with general drive systems. Finally, we apply the proposed method to design two underactuated TDMs and demonstrate that the proposed method guarantees a nonsingular series actuation transmission and that the designed underactuated TDMs could achieve arbitrary stiffness independent of the actuation effort compared with the conventional underactuated TDM with torsion springs.

Section II presents the basic kinematics of the transmissions and defines TDMs. Section III classifies TDMs into six classes based on their controllability and driving DOF. In Section IV, the bias forces of the TDMs are analyzed to investigate the bias force independence and the separability of the TDMs into smaller TDMs. Section V proposes a design method for TDMs based on their separability. In Section VI, we design a number of mechanisms and validate the effectiveness of the proposed design method.

II. Basic Kinematics of Tendon-Driven Mechanisms

A. Kinematics of Transmission

First, we consider two basic tendon types: passive and active. Passive tendons are connected to an elastic element instead of an actuator, as shown in Fig. 1(a). These tendons require pretension to prevent them from losing tension, and this pretension cannot be adjusted during motion. Therefore, the tension of passive tendons depends on the configuration of the robotic system. Active tendons are connected to an actuator, as shown in Fig. 1(b). These active tendons are permitted to have an elastic element in series [12], [21], [22] because the actuator can adjust the tension of the active tendon during motion, despite the presence or absence of the elastic element. Let $\boldsymbol{l} \in \mathbb{R}^L$, $\boldsymbol{\theta} = (\theta_1, \theta_2, \ldots, \theta_M) \in \mathbb{R}^M$, and $\boldsymbol{q} = (q_1, q_2, \ldots, q_N) \in \mathcal{Q} \subset \mathbb{R}^N$ be the tendon stretch, the actuator rotation angle, and joint angle vectors, respectively, where L, M, and N are the numbers of tendons, actuators, and joints of the system, respectively. The relationship among $\boldsymbol{l}, \boldsymbol{q}$, and $\boldsymbol{\theta}$ is given as follows:

$$\boldsymbol{l} = \boldsymbol{l}(\boldsymbol{q}, \boldsymbol{\theta}, \boldsymbol{l}_0) = \begin{bmatrix} \boldsymbol{l}_a(\boldsymbol{q}, \boldsymbol{\theta}) \\ \boldsymbol{l}_e(\boldsymbol{q}, \boldsymbol{l}_0) \end{bmatrix}. \tag{1}$$

$\boldsymbol{l}_0 > \boldsymbol{0} \in \mathbb{R}^{L-M}$ is the initial stretch of the passive tendons. $\boldsymbol{l}_a \in \mathbb{R}^M$ is the stretch of the active tendons, which depends on $\boldsymbol{q}$ and $\boldsymbol{\theta}$ if a series elastic element is installed; otherwise, it is zero. $\boldsymbol{l}_e \in \mathbb{R}^{L-M}$ is the stretch of the passive tendons, which depends on $\boldsymbol{q}$ and $\boldsymbol{l}_0$. We call (1) a tendon transmission mechanism. The time derivative of the tendon stretch is given as follows:

$$\dot{\boldsymbol{l}} = \boldsymbol{J}_j \dot{\boldsymbol{q}} + \begin{bmatrix} \boldsymbol{R}_a \\ \boldsymbol{0} \end{bmatrix} \dot{\boldsymbol{\theta}}, \text{where } \boldsymbol{J}_j = \begin{bmatrix} \boldsymbol{J}_a \\ \boldsymbol{J}_e \end{bmatrix}. \tag{2}$$

$\boldsymbol{J}_j$ is the tendon Jacobian and $\boldsymbol{J}_a$ and $\boldsymbol{J}_e$ are the active and passive tendon Jacobians, respectively. $\boldsymbol{R}_a$ is the diagonal matrix, whose diagonal elements are the pulley radii attached on the actuators. Then, from the virtual work principle, the joint torque $\boldsymbol{\tau} \in \mathcal{T} \subset \mathbb{R}^N$ of this mechanism is given as follows:

$$\boldsymbol{\tau} = -\boldsymbol{J}_j^{\mathrm{T}} \boldsymbol{f}_t. \tag{3}$$

The tensile force can be rewritten using (3) as follows:

$$\boldsymbol{f}_t = \boldsymbol{A}_1 \boldsymbol{\tau} + \boldsymbol{f}_b \tag{4}$$

where $\boldsymbol{A}_1$ is the generalized inverse of $-\boldsymbol{J}_j^{\mathrm{T}}$, which is defined as $\boldsymbol{A}_1 = -(\boldsymbol{J}_j^{\mathrm{T}})^+$ when rank $\boldsymbol{J}_j^{\mathrm{T}} = N$. $\boldsymbol{f}_b = (\boldsymbol{f}_{ba}, \boldsymbol{f}_{be})$ is a vector that satisfies $\boldsymbol{J}_j^{\mathrm{T}} \boldsymbol{f}_b = \boldsymbol{0}$, and $\boldsymbol{f}_{ba}$ and $\boldsymbol{f}_{be}$ are vectors corresponding to the active and the passive tendons, respectively.

B. Equilibrium Points and Tendon-Driven Mechanisms

First, we make the following assumptions to discuss the equilibrium point of a mechanism:

1) The range $\mathcal{Q}$ of the joint angle $\boldsymbol{q}$ is bounded.
2) The range $\mathcal{T}$ of the joint torque $\boldsymbol{\tau}$ is bounded.
3) The initial tension of the passive tendons is great enough to prevent slack.
4) The actuator power is great enough to generate arbitrary torque $\boldsymbol{\tau} \in \mathcal{T}$.
5) Any tendons in a mechanism are not parallel [20][1].
6) The tensile forces of tendons are proportional to the stretches resulting from the inherent elasticity of the passive tendons or the feedback of the active tendons, where $\boldsymbol{\theta}$ is regarded as a virtual actuator rotation angle if an active tendon is nonelastic. The tensile force $\boldsymbol{f}_t$ can then be described as

$$\boldsymbol{f}_t = \begin{bmatrix} \boldsymbol{f}_{ta} \\ \boldsymbol{f}_{te} \end{bmatrix} = \begin{bmatrix} \boldsymbol{K}_a \boldsymbol{l}_a(\boldsymbol{q}, \boldsymbol{\theta}) \\ \boldsymbol{K}_e \boldsymbol{l}_e(\boldsymbol{q}, \boldsymbol{l}_0) \end{bmatrix} \tag{5}$$

   where $\boldsymbol{K}_a$ and $\boldsymbol{K}_e$ are the stiffness matrices of the active and passive tendons, respectively, which are positive definite matrices.
7) The friction from wrapping around the pulleys does not affect tendon elongation.

[1]Two arbitrary row vectors $\boldsymbol{r}$ and $\boldsymbol{s}$ in $\boldsymbol{J}_j$ are referred to as parallel when $\boldsymbol{r} = \alpha \boldsymbol{s}$, where α is a positive constant.

From (3) and (5), the joint torque $\boldsymbol{\tau}$ is determined by the joint angle $\boldsymbol{q}$, the actuator angle $\boldsymbol{\theta}$, and the initial stretch of the passive tendon $\boldsymbol{l}_0$ as follows:

$$\boldsymbol{\tau} = -\boldsymbol{J}_a^{\mathrm{T}} \boldsymbol{K}_a (\boldsymbol{J}_a \boldsymbol{q} + \boldsymbol{R}_a \boldsymbol{\theta}) - \boldsymbol{J}_e^{\mathrm{T}} \boldsymbol{K}_e (\boldsymbol{J}_e \boldsymbol{q} + \boldsymbol{l}_0). \quad (6)$$

Therefore, the triple $\boldsymbol{x} = \{\boldsymbol{q}, \boldsymbol{\theta}, \boldsymbol{l}_0\}$ is the state of the tendon transmission mechanism (1). Then, we have the following definitions and proposition:

Definition 2.1: The state $\boldsymbol{x} = \{\boldsymbol{q}, \boldsymbol{\theta}, \boldsymbol{l}_0\}$ is called an equilibrium point of the tendon transmission mechanism (1) if the joint torque $\boldsymbol{\tau}$ is zero and all the elements of the tensile force $\boldsymbol{f}_t$ are positive at $\boldsymbol{x}$.

Definition 2.2: A tendon transmission mechanism (1) is a TDM if the mechanism has equilibrium points. Otherwise, the mechanism is a nontendon-drivable mechanism.

Proposition 2.1: A tendon transmission mechanism is a TDM if and only if there exists a positive bias force $\boldsymbol{f}_b$.

The proof of Proposition II.1 is trivial; therefore, we omit it. Here, we define two classes of TDMs as follows:

Definition 2.3: A TDM is called a pulley-routed TDM if $\boldsymbol{J}_j$ is constant. Otherwise, a TDM is called a suspended TDM.

The moment arms of the tensile force in suspended TDMs depend on joint configurations [15], [16], [23] and, in contrast, those of pulley-routed TDMs are always constant because of the circular pulleys mounted on the joints.[2] In this case, the mechanism (1) is rewritten as follows:

$$\boldsymbol{l} = \boldsymbol{J}_j \boldsymbol{q} + \boldsymbol{g}(\boldsymbol{\theta}, \boldsymbol{l}_0) = \begin{bmatrix} \boldsymbol{J}_a \\ \boldsymbol{J}_e \end{bmatrix} \boldsymbol{q} + \begin{bmatrix} \boldsymbol{R}_a \boldsymbol{\theta} \\ \boldsymbol{l}_0 \end{bmatrix}. \quad (7)$$

Hereafter, we only treat pulley-routed TDMs and we also call them TDMs when it is trivial to do so.

III. Classification of Tendon-Driven Mechanisms

We will discuss how TDMs are classified into several groups according to their controllability and driving DOF in the following sections.

A. Controllable Tendon-Driven Mechanisms

First, we define a stable equilibrium point as follows:

Definition 3.1: If the torque generated by any infinitesimal joint displacement returns the state to the equilibrium point $\boldsymbol{x}_0 = \{\boldsymbol{q}_0, \boldsymbol{\theta}_0, \boldsymbol{l}_0\}$, then $\boldsymbol{x}_0$ is a stable equilibrium point.

TDMs can be classified into two mechanisms based on a stable equilibrium point as follows:

Definition 3.2: TDMs are called controllable tendon-driven mechanisms (C-TDMs) if there exists a stable equilibrium point. Otherwise, the TDMs are called uncontrollable tendon-driven mechanisms (U-TDMs).

The following proposition is useful in identifying the above mechanisms:

Proposition 3.1:

1) A TDM is a C-TDM if and only if there exists a positive bias force $\boldsymbol{f}_b > \boldsymbol{0}$ and rank $\boldsymbol{J}_j = N$.
2) A TDM is a U-TDM if and only if there exists a positive bias force $\boldsymbol{f}_b > \boldsymbol{0}$ and rank $\boldsymbol{J}_j < N$.

The proof will be described in Appendix A.

Let $\boldsymbol{x}_0 = \{\boldsymbol{q}_0, \boldsymbol{\theta}_0, \boldsymbol{l}_0\}$ be the equilibrium point. The torque at the equilibrium point becomes zero as follows:

$$\boldsymbol{J}_a^{\mathrm{T}} \boldsymbol{K}_a (\boldsymbol{J}_a \boldsymbol{q}_0 + \boldsymbol{R}_a \boldsymbol{\theta}_0) + \boldsymbol{J}_e^{\mathrm{T}} \boldsymbol{K}_e (\boldsymbol{J}_e \boldsymbol{q}_0 + \boldsymbol{l}_0) = \boldsymbol{0}. \quad (8)$$

Then, the tensile force $\boldsymbol{f}_t$ equals the bias force $\boldsymbol{f}_b$. Substituting (7) into (5), we obtain the following equations:

$$\boldsymbol{f}_t = \begin{bmatrix} \boldsymbol{K}_a (\boldsymbol{J}_a \boldsymbol{q} + \boldsymbol{R}_a \boldsymbol{\theta}) \\ \boldsymbol{K}_e (\boldsymbol{J}_e \boldsymbol{q} + \boldsymbol{l}_0) \end{bmatrix} = \begin{bmatrix} \boldsymbol{f}_{ba} \\ \boldsymbol{f}_{be} \end{bmatrix} > \boldsymbol{0}. \quad (9)$$

Thus, the equilibrium point can be expressed as follows:

$$\begin{aligned} \boldsymbol{\theta}_0 &= \boldsymbol{R}_a^{-1} (\boldsymbol{K}_a^{-1} \boldsymbol{f}_{ba} - \boldsymbol{J}_a \boldsymbol{q}_0), \\ \boldsymbol{l}_0 &= \boldsymbol{K}_e^{-1} \boldsymbol{f}_{be} - \boldsymbol{J}_e \boldsymbol{q}_0, \end{aligned} \quad (10)$$

where the following inequalities are satisfied to keep the tensions positive

$$\boldsymbol{J}_e \boldsymbol{q}_0 > -\boldsymbol{l}_0 \text{ and } \boldsymbol{R}_a \boldsymbol{\theta}_0 > -\boldsymbol{J}_a \boldsymbol{q}_0. \quad (11)$$

We consider another equilibrium point $\boldsymbol{x} = \{\boldsymbol{q}, \boldsymbol{\theta}, \boldsymbol{l}_0\}$. Thus,

$$\boldsymbol{J}_a^{\mathrm{T}} \boldsymbol{K}_a (\boldsymbol{J}_a \boldsymbol{q} + \boldsymbol{R}_a \boldsymbol{\theta}) + \boldsymbol{J}_e^{\mathrm{T}} \boldsymbol{K}_e (\boldsymbol{J}_e \boldsymbol{q} + \boldsymbol{l}_0) = \boldsymbol{0} \quad (12)$$

where $\boldsymbol{x}$ must also satisfy

$$\boldsymbol{J}_e \boldsymbol{q} > -\boldsymbol{l}_0, \text{ and } \boldsymbol{R}_a \boldsymbol{\theta} > -\boldsymbol{J}_j \boldsymbol{q}. \quad (13)$$

Subtracting (8) from (12), we have

$$\boldsymbol{J}_a^{\mathrm{T}} \boldsymbol{K}_a (\boldsymbol{J}_a \Delta\boldsymbol{q} + \boldsymbol{R}_a \Delta\boldsymbol{\theta}) + \boldsymbol{J}_e^{\mathrm{T}} \boldsymbol{K}_e \boldsymbol{J}_e \Delta\boldsymbol{q} = \boldsymbol{0} \quad (14)$$

where $\Delta\boldsymbol{q} = \boldsymbol{q} - \boldsymbol{q}_0$ and $\Delta\boldsymbol{\theta} = \boldsymbol{\theta} - \boldsymbol{\theta}_0$. Then

$$\boldsymbol{q} = -(\boldsymbol{J}_a^{\mathrm{T}} \boldsymbol{K}_a \boldsymbol{J}_a + \boldsymbol{J}_e^{\mathrm{T}} \boldsymbol{K}_e \boldsymbol{J}_e)^{-1} \boldsymbol{J}_a \boldsymbol{K}_a \boldsymbol{R}_a \Delta\boldsymbol{\theta} + \boldsymbol{q}_0. \quad (15)$$

This means that the set of the equilibrium points is given as follows:

$$\mathcal{T}(\boldsymbol{l}_0) = \{(\boldsymbol{q}, \boldsymbol{\theta}, \boldsymbol{l}_0) | (10), (15), \text{and } (13), \boldsymbol{\theta} \in \mathbb{R}^L\}. \quad (16)$$

For the bounded $\boldsymbol{q}$, $\boldsymbol{\theta}$ can be made to satisfy (13) by making $\boldsymbol{f}_{ba}$ and $\boldsymbol{f}_{be}$ large enough with (10). Therefore, in a qualitative discussion, these constraints can be neglected, and $\mathcal{T}_\infty$ is called a controllable affine subspace of TDMs and is given as follows:

$$\mathcal{T}_\infty = \mathrm{Re}\{(\boldsymbol{J}_a^{\mathrm{T}} \boldsymbol{K}_a \boldsymbol{J}_a + \boldsymbol{J}_e^{\mathrm{T}} \boldsymbol{K}_e \boldsymbol{J}_e)^{-1} \boldsymbol{J}_a^{\mathrm{T}}\} + \boldsymbol{q}_0 \quad (17)$$

where $\mathrm{Re}(\boldsymbol{A})$ is the range of $\boldsymbol{A}$. Then, we have

$$\dim \mathcal{T}_\infty = \mathrm{rank}\, \boldsymbol{J}_a. \quad (18)$$

Therefore, the rank of $\boldsymbol{J}_a$ determines the independent joint variable number, and C-TDMs are classified as follows:

Definition 3.3 [Controllable full/semi/passive-tendon-driven mechanism (CF/CS/CP-TDM)]: [3]

1) In the case where rank $\boldsymbol{J}_a = N$, the C-TDM is a controllable full-tendon-driven mechanism (CF-TDM).
2) In the case where rank $\boldsymbol{J}_a = 0$, the C-TDM is a controllable passive-tendon-driven mechanism (CP-TDM).

[2] As an exception, if the pulleys of a TDM are noncircular, then the TDM is categorized as a suspended TDM, even though the TDM uses pulleys.

[3] In [7], CF-TDMs and CS-TDMs are referred to as tendon-controllable and hybrid active/passive tendon-driven mechanisms, respectively.

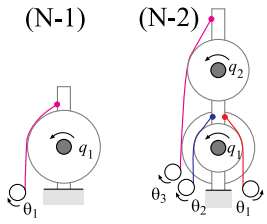

Fig. 2. Examples of nontendon-drivable mechanisms.

TABLE I
PROPERTY OF NONTENDON-DRIVABLE MECHANISMS IN FIG. 2

	$\boldsymbol{J}_j$	$\boldsymbol{f}_b$	N	rank $\boldsymbol{J}_j$	rank $\boldsymbol{J}_a$
N-1	$\boldsymbol{J}_a = \begin{bmatrix} -1 \end{bmatrix}$	none	1	1	1
N-2	$\boldsymbol{J}_a = \begin{bmatrix} 1 & 0 \\ -1 & 0 \\ -1 & -1 \end{bmatrix}$	none	2	2	2

3) Otherwise, the C-TDM is a controllable semi-tendon-driven mechanism (CS-TDM).

A CF-TDM coincides with a conventional TDM that can actuate all its joints independently. A CS-TDM is driven by fewer actuator DOF than the number of joints and is frequently used for prosthetic and robotic hands that adaptively grasp an object using their palms. A CP-TDM is a type of a remote compliance center [24] and does not have any actuators.

B. Uncontrollable Tendon-Driven Mechanisms

U-TDMs are classified into three submechanisms by a discussion similar to *Definition III.3* as follows:

Definition 3.4 [Uncontrollable full/semi/passive-tendon-driven mechanism (UF/US/UP-TDM)]:

1) In the case where rank $\boldsymbol{J}_a = \text{rank}\, \boldsymbol{J}_j < N$, the U-TDM is an uncontrollable full-tendon-driven mechanism (UF-TDM).
2) In the case where rank $\boldsymbol{J}_a = 0$, the U-TDM is an uncontrollable passive-tendon-driven mechanism (UP-TDM).
3) Otherwise, the U-TDM is an uncontrollable semi-tendon-driven mechanism (US-TDM).

Example 3.1: Figs. 2–4 provide examples of tendon transmission mechanisms whose Jacobians, bias forces, DOF, and Jacobian ranks are listed in Tables I–III, respectively, where the radii of all the pulleys are assumed to be unified for the sake of simplicity. The mechanisms in Fig. 2 (N-1) and (N-2) cannot rotate the first and the second joints, respectively, in the clockwise direction. Therefore, these mechanisms are nontendon-drivable mechanisms.

All the mechanisms in Fig. 3 are C-TDMs because each mechanism has a positive bias force and its rank of $\boldsymbol{J}_j$ equals N, as shown in Table II. The mechanisms (CF-1 to 4), (CS-1 to 4), and (CP-1, 2) are examples of CF-TDMs, CS-TDMs, and CP-TDMs, respectively, because of the rank of $\boldsymbol{J}_a$.

All the mechanisms in Fig. 4 are U-TDMs because these mechanisms satisfy the conditions $\boldsymbol{f}_b > \boldsymbol{0}$ and rank $\boldsymbol{J}_j < N$, as shown in Table III. The mechanisms (UF-1 to 4) are UF-TDMs because rank $\boldsymbol{J}_a = \text{rank}\, \boldsymbol{J}_j$. The mechanisms (US-1 to 3)

TABLE II
PROPERTY OF C-TDMS IN FIG. 3

	$\boldsymbol{J}_j$	$\boldsymbol{f}_b$	N	rank $\boldsymbol{J}_j$	rank $\boldsymbol{J}_a$
CF-1	$\boldsymbol{J}_a = \begin{bmatrix} 1 \\ -1 \end{bmatrix}$	$\begin{bmatrix} 1 \\ 1 \end{bmatrix}$	1	1	1
CF-2	$\boldsymbol{J}_a = \begin{bmatrix} 1 & 1 \\ 1 & -1 \\ -1 & 0 \end{bmatrix}$	$\begin{bmatrix} 1 \\ 1 \\ 2 \end{bmatrix}$	2	2	2
CF-3	$\begin{bmatrix} \boldsymbol{J}_a \\ \boldsymbol{J}_e \end{bmatrix} = \left[\begin{array}{cc} 1 & 1 \\ 1 & -1 \\ \hdashline -1 & 0 \end{array}\right]$	$\begin{bmatrix} 1 \\ 1 \\ 2 \end{bmatrix}$	2	2	2
CF-4	$\boldsymbol{J}_a = \begin{bmatrix} 1 & 1 \\ 1 & -1 \\ -1 & 0 \\ -1 & -1 \end{bmatrix}$	$\begin{bmatrix} 2 \\ 1 \\ 2 \\ 1 \end{bmatrix}$	2	2	2
CS-1	$\begin{bmatrix} \boldsymbol{J}_a \\ \boldsymbol{J}_e \end{bmatrix} = \left[\begin{array}{cc} 1 & 1 \\ \hdashline 1 & -1 \\ -1 & 0 \end{array}\right]$	$\begin{bmatrix} 1 \\ 1 \\ 2 \end{bmatrix}$	2	2	1
CS-2	$\begin{bmatrix} \boldsymbol{J}_a \\ \boldsymbol{J}_e \end{bmatrix} = \left[\begin{array}{cc} 1 & 1 \\ -1 & -1 \\ \hdashline 1 & 0 \\ -1 & 0 \end{array}\right]$	$\begin{bmatrix} 1 \\ 1 \\ 1 \\ 1 \end{bmatrix}$	2	2	1
CS-3	$\begin{bmatrix} \boldsymbol{J}_a \\ \boldsymbol{J}_e \end{bmatrix} = \left[\begin{array}{cc} 1 & 1 \\ -1 & -1 \\ \hdashline 1 & -1 \\ -1 & 1 \end{array}\right]$	$\begin{bmatrix} 1 \\ 1 \\ 1 \\ 1 \end{bmatrix}$	2	2	1
CS-4	$\begin{bmatrix} \boldsymbol{J}_a \\ \boldsymbol{J}_e \end{bmatrix} = \left[\begin{array}{cc} 1 & 1 \\ -1 & -1 \\ \hdashline -1 & 1 \\ 1 & -1 \\ 1 & 0 \\ -1 & 0 \end{array}\right]$	$\begin{bmatrix} 1 \\ 1 \\ 1 \\ 1 \\ 1 \\ 1 \end{bmatrix}$	2	2	1
CP-1	$\boldsymbol{J}_e = \begin{bmatrix} 1 & 1 \\ 1 & -1 \\ -1 & 0 \end{bmatrix}$	$\begin{bmatrix} 1 \\ 1 \\ 2 \end{bmatrix}$	2	2	0
CP-2	$\boldsymbol{J}_e = \begin{bmatrix} 1 & 0 \\ -1 & 0 \\ 0 & 1 \\ 0 & -1 \end{bmatrix}$	$\begin{bmatrix} 1 \\ 1 \\ 1 \\ 1 \end{bmatrix}$	2	2	0

TABLE III
PROPERTY OF U-TDMS IN FIG. 4

	$\boldsymbol{J}_j$	$\boldsymbol{f}_b$	N	rank $\boldsymbol{J}_j$	rank $\boldsymbol{J}_a$
UF-1	$\boldsymbol{J}_a = \begin{bmatrix} 1 & 0 \\ -1 & 0 \end{bmatrix}$	$\begin{bmatrix} 1 \\ 1 \end{bmatrix}$	2	1	1
UF-2	$\boldsymbol{J}_a = \begin{bmatrix} 1 & 1 \\ -1 & -1 \end{bmatrix}$	$\begin{bmatrix} 1 \\ 1 \end{bmatrix}$	2	1	1
UF-3	$\begin{bmatrix} \boldsymbol{J}_a \\ \boldsymbol{J}_e \end{bmatrix} = \left[\begin{array}{cc} 1 & 1 \\ \hdashline -1 & -1 \end{array}\right]$	$\begin{bmatrix} 1 \\ 1 \end{bmatrix}$	2	1	1
UF-4	$\boldsymbol{J}_a = \begin{bmatrix} 1 & 1 & 1 \\ -1 & -1 & -1 \end{bmatrix}$	$\begin{bmatrix} 1 \\ 1 \end{bmatrix}$	3	1	1
US-1	$\begin{bmatrix} \boldsymbol{J}_a \\ \boldsymbol{J}_e \end{bmatrix} = \left[\begin{array}{ccc} 1 & 1 & 1 \\ \hdashline 1 & -1 & -1 \\ -1 & 0 & 0 \end{array}\right]$	$\begin{bmatrix} 1 \\ 1 \\ 2 \end{bmatrix}$	3	2	1
US-2	$\begin{bmatrix} \boldsymbol{J}_a \\ \boldsymbol{J}_e \end{bmatrix} = \left[\begin{array}{ccc} 1 & 1 & 1 \\ -1 & -1 & -1 \\ \hdashline 1 & 0 & 0 \\ -1 & 0 & 0 \end{array}\right]$	$\begin{bmatrix} 1 \\ 1 \\ 1 \\ 1 \end{bmatrix}$	3	2	1
US-3	$\begin{bmatrix} \boldsymbol{J}_a \\ \boldsymbol{J}_e \end{bmatrix} = \left[\begin{array}{ccc} 1 & 1 & 0 \\ -1 & -1 & 0 \\ \hdashline 0 & -1 & 1 \\ 0 & 1 & -1 \end{array}\right]$	$\begin{bmatrix} 1 \\ 1 \\ 1 \\ 1 \end{bmatrix}$	3	2	1
UP-1	$\boldsymbol{J}_e = \begin{bmatrix} 1 & 0 \\ -1 & 0 \end{bmatrix}$	$\begin{bmatrix} 1 \\ 1 \end{bmatrix}$	2	1	0
UP-2	$\boldsymbol{J}_e = \begin{bmatrix} 1 & -1 \\ -1 & 1 \end{bmatrix}$	$\begin{bmatrix} 1 \\ 1 \end{bmatrix}$	2	1	0
UP-3	$\boldsymbol{J}_e = \begin{bmatrix} 0 & -1 & 1 \\ 0 & 1 & -1 \end{bmatrix}$	$\begin{bmatrix} 1 \\ 1 \end{bmatrix}$	3	1	0
UP-4	$\boldsymbol{J}_e = \begin{bmatrix} 0 & -1 & 1 \\ 0 & 1 & -1 \\ 1 & -1 & 0 \\ -1 & 1 & 0 \end{bmatrix}$	$\begin{bmatrix} 1 \\ 1 \\ 1 \\ 1 \end{bmatrix}$	3	2	0

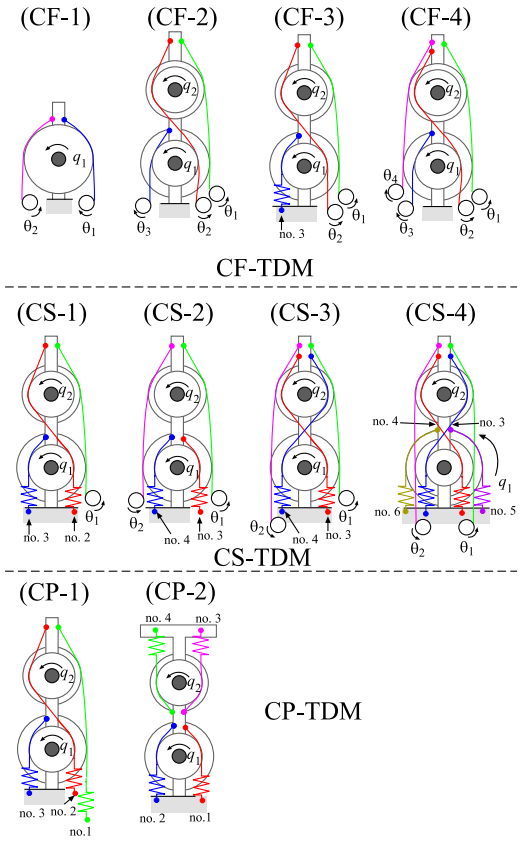

Fig. 3. Examples of C-TDMs. Controllable Full-TDMs (CF-1 to 4). Controllable Semi-TDMs (CS-1 to 4). Controllable Passive-TDMs (CP-1 to 2).

TABLE IV
CLASSIFICATION OF TDMS

	rank $\boldsymbol{J}_a$ = rank $\boldsymbol{J}_j$	rank $\boldsymbol{J}_a$ = 0	rank $\boldsymbol{J}_a$ otherwise
rank $\boldsymbol{J}_j = N$	CF-TDM	CP-TDM	CS-TDM
rank $\boldsymbol{J}_j < N$	UF-TDM	UP-TDM	US-TDM

We can classify a pulley-routed tdm into six classes according to the ranks of $\boldsymbol{j}_j$ and $\boldsymbol{j}_a$.

are US-TDMs because rank $\boldsymbol{J}_a <$ rank $\boldsymbol{J}_j$. The mechanisms (UP-1 to 4) are UP-TDMs because rank $\boldsymbol{J}_a = 0$.

Fig. 5 shows the classification of the TDMs. Each TDM is differentiated by the conditions on the left, which are in Table IV.

Finally, Table V categorizes the finger mechanisms developed using TDMs and other drive systems in terms of controllability and actuation, where other drive systems are referred to as CF/CS/UF-mechanisms, similar to CF/CS/UF-TDMs.

Most of the UF/CS-TDMs were developed to adaptively grasp an object with a palm and were originally proposed as soft gripper mechanisms [3]. UF-TDMs cannot grasp an object with a fingertip, while CS-TDMs can, representing an important difference in the design of robotic hands. However, both UF/CS-TDMs are frequently referred to as underactuated mechanisms without distinction [8]. In contrast, UP-TDMs have limited applications but play an important role in designing CS-TDMs, together with UF-TDMs, in Section V.

The following theorem is important in analyzing TDMs.

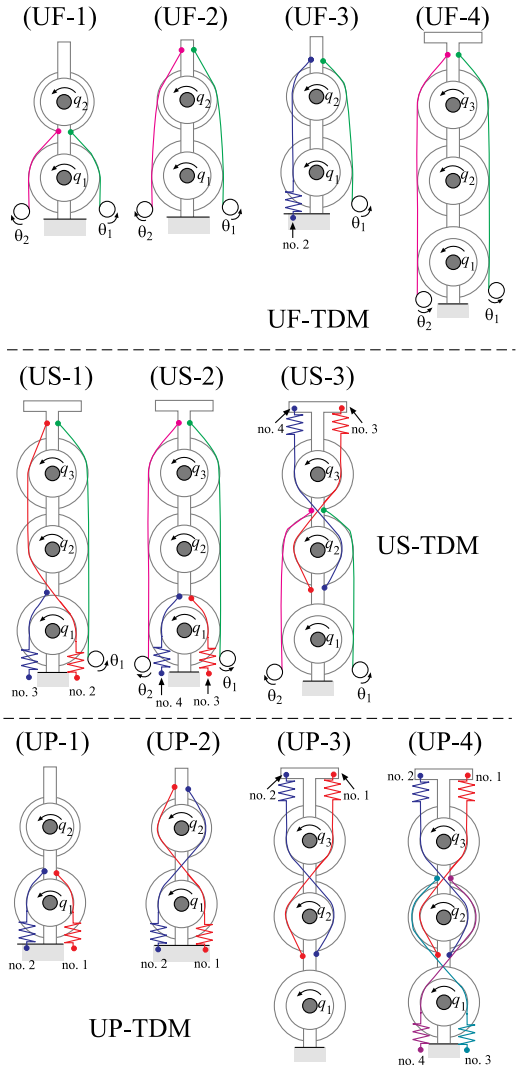

Fig. 4. Examples of U-TDMs. Uncontrollable Full Tendon-Driven Mechanism (UF-1 to 4). Uncontrollable Semitendon-Driven Mechanism (US-1 to 3). Uncontrollable Passive-Tendon-Driven Mechanism (UP-1 to 4).

Theorem 3.1: The controllability of a TDM is invariant under the following transformations [20]:

1) when multiplying a nonsingular matrix from the right-hand side of $\boldsymbol{J}_j$;
2) when changing the order of the rows of $\boldsymbol{J}_j$;
3) when multiplying a positive constant with a row vector of $\boldsymbol{J}_j$.

Tranformation 1 corresponds to mapping the joint space to an appropriate homeomorphic space. Tranformation 2 and 3 correspond to changing the order of the tendons and to changing all the pulley radii of the corresponding tendon by the same rate, respectively. These transformations are expressed as follows:

$$\boldsymbol{J}_j = \boldsymbol{PWT} \tag{19}$$

where $\boldsymbol{P} \in \mathbb{R}^{L\times L}$ is a positive matrix, $\boldsymbol{W} \in \mathbb{R}^{L\times N}$ a tendon Jacobian, and $\boldsymbol{T} \in \mathbb{R}^{N\times N}$ a nonsingular matrix corresponding to tranformation 1. If the order of the tendons is appropriately changed, which corresponds to tranformation 2, then $\boldsymbol{P}$ becomes a positive diagonal matrix, which corresponds to tranformation 3.

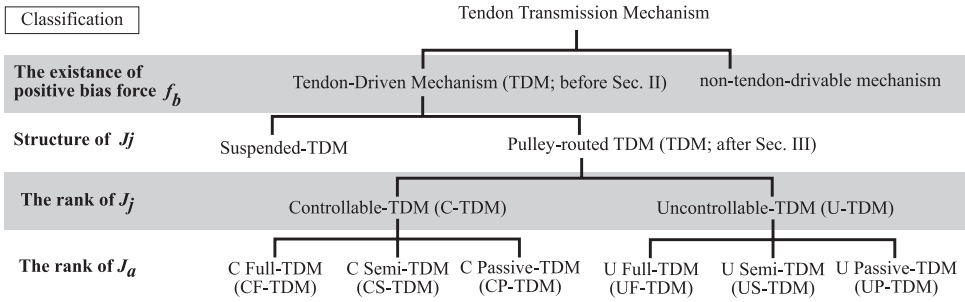

Fig. 5. Classifications and design of TDMs in terms of the controllability and drivability.

TABLE V
CATEGORIZATION OF ROBOTIC INDEX FINGERS

Conventional methods	The proposed method	TDMs	Bilateral mechanisms	TDMs+ bilateral mechanisms
Full-actuated	CF-TDM (CF-mechanism)	Salisbury(Stanford/JPL hand)[13] Jacobsen(UTAH/MIT Hand)[14] Kobayashi[25], [21] Ogane [12] Lee(POSTECH Hand II) [26]	Namiki [27]	
Under-actuated	CS-TDM (CS-mechanism)	Ozawa[7]	Dechev[28] Townsend(BarrettHand)[29] Fukaya(TUAT/Karlsruhe)[30] Kawasaki(Gifu Hand)[31] Liu(DLR Hand) [32] Liu(DLR-HIT Hand) [9] Pons(MANUS-Hand) [33] Koganezawa [10] Figliolini[4] Zhao[2]	Massa[34] Cabas[35] Krut[36] Higashimori [37] Lotti(UB Hand 3)[38] Mizuuchi [16]
	UF-TDM (UF-mechanism)	Hirose(Soft Gripper)[3] Kaneko(100G Capturing Hand)[6]	Figliolini[5]	

IV. BIAS FORCE BASIS AND SUBTENDON-DRIVEN MECHANISMS

In this section, we discuss the conditions required to decompose a TDM into several smaller TDMs according to the independence and orthogonality of the bias force.

First, we define a set of nonnegative vectors as follows:

Definition 4.1: If, using mutually independent nonnegative vectors $\boldsymbol{f}_{bk}$ $(k = 1, 2, \ldots, s)$ satisfying $\boldsymbol{J}_j^{\mathrm{T}} \boldsymbol{f}_{bk} = \boldsymbol{0}$, a bias force $\boldsymbol{f}_b$ of a TDM can be expressed as

$$\boldsymbol{f}_b = \boldsymbol{f}_{b1} + \boldsymbol{f}_{b2} + \cdots + \boldsymbol{f}_{bs} > \boldsymbol{0} \tag{20}$$

then $\boldsymbol{f}_{bk}$ is called a sub-bias force of $\boldsymbol{f}_b$.

When the order of the tendon is changed appropriately, the sub-bias force $\boldsymbol{f}_{bk}$ can be rewritten as follows:

$$\boldsymbol{f}_{bk} = \begin{bmatrix} \boldsymbol{0} \\ \bar{\boldsymbol{f}}_{bk} \\ \boldsymbol{0} \end{bmatrix} \tag{21}$$

where $\bar{\boldsymbol{f}}_{bk} > \boldsymbol{0}$ is the vector that collected only the positive elements of $\boldsymbol{f}_{bk}$. Then, the mechanism with the tendons corresponding to $\bar{\boldsymbol{f}}_{bk}$ is described as follows:

$$\boldsymbol{l}_k = \boldsymbol{J}_{jk}\boldsymbol{q} + \boldsymbol{g}_k(\boldsymbol{\theta}_k, \boldsymbol{l}_{0k}) \text{ for } k = 1, 2, \ldots, s \tag{22}$$

where $\boldsymbol{l}_k \in \mathbb{R}^{L_k}$ and $\boldsymbol{J}_{jk} \in \mathbb{R}^{L_k \times N}$ are the tendon stretch and the Jacobian, respectively, corresponding to $\bar{\boldsymbol{f}}_{bk}$. $\bar{\boldsymbol{f}}_{bk}$ is clearly the bias force to the mechanism (22) that can be defined as follows:

*Definition 4.2 [Subtendon-driven mechanism]:*The mechanism (22) is a TDM and is called a subtendon-driven mechanism (SubTDM).

Example 4.1: The bias force of the TDM (CF-4) in Fig. 3 consists of two sub-bias forces as follows:

$$\boldsymbol{f}_{b1} = \begin{bmatrix} 1 \\ 1 \\ 2 \\ 0 \end{bmatrix}, \text{ and } \boldsymbol{f}_{b2} = \begin{bmatrix} 1 \\ 0 \\ 0 \\ 1 \end{bmatrix}. \tag{23}$$

The TDM (CF-4) is regarded as the combination of the SubTDMs in Fig. 3 (CF-2) and Fig. 4 (UF-2).

Note that if we separate the tendons of (CF-4) into two groups, at least one of the resulting sub-mechanisms is not a SubTDM. Therefore, (CF-4) is not separable into two SubTDMs. On the other hand, (CS-2) can be separated into two independent SubTDMs (UF-2) and (UP-1).

To guarantee the separability of TDMs, we need the following proposition:

Proposition 4.1: A TDM with the bias force expressed in (20) is separable to s SubTDMs (22) if the tendon Jacobian $\boldsymbol{J}_j$ can be expressed with the combination of the tendon Jacobians

$\boldsymbol{J}_{jk}(k = 1, 2, \ldots, s)$ of the SubTDMs as follows:

$$\boldsymbol{J}_j = \begin{bmatrix} \boldsymbol{J}_{j1} \\ \boldsymbol{J}_{j2} \\ \vdots \\ \boldsymbol{J}_{js} \end{bmatrix}. \tag{24}$$

The proof of Proposition IV.1 will be described in Appendix B.

From (24), a separable TDM clearly satisfies

$$\text{rank } \boldsymbol{J}_j \leq \sum_{k=1}^{s} \text{rank } \boldsymbol{J}_{jk}. \tag{25}$$

It is important to consider a class of separable TDMs as follows:

Definition 4.3: A separable TDM satisfying the condition

$$\text{rank } \boldsymbol{J}_j = \sum_{k=1}^{s} \text{rank } \boldsymbol{J}_{jk} \tag{26}$$

is called a decoupled TDM.

Example 4.2: (CS-2) and (CS-3) are decoupled TDMs. (CS-4) is separable but not decoupled.

To clarify the meaning of a decoupled TDM, we introduce a property of tendon Jacobian $\boldsymbol{J}_{jk}$ using the similarity of (19) as follows:

$$\boldsymbol{J}_{jk} = \bar{\boldsymbol{P}}_k \bar{\boldsymbol{W}}_k \bar{\boldsymbol{T}}_k \tag{27}$$

where $\bar{\boldsymbol{P}}_k \in \mathbb{R}^{L_k \times L_k}$ is the positive diagonal matrix used to adjust the pulley radius of the tendon, $\bar{\boldsymbol{W}}_k \in \mathbb{R}^{L_k \times \lambda_k}$ is a canonical tendon Jacobian discussed later in Section V-C, and $\bar{\boldsymbol{T}}_k \in \mathbb{R}^{\lambda_k \times N}$ is an appropriate matrix with full column-rank λ_k.

By substituting (27) into (22), each SubTDM of a decoupled TDM is rewritten as follows:

$$\boldsymbol{l}_k = \bar{\boldsymbol{P}}_k \bar{\boldsymbol{W}}_k \bar{\boldsymbol{q}}_k + \boldsymbol{g}_k(\boldsymbol{\theta}_k, \boldsymbol{l}_{0k}) \text{ for } k = 1, 2, \ldots, s \tag{28}$$

where

$$\bar{\boldsymbol{q}}_k = \bar{\boldsymbol{T}}_k \boldsymbol{q}. \tag{29}$$

$\bar{\boldsymbol{q}}_k \in \mathbb{R}^{\lambda_k}$ is decoupled from the other SubTDMs and is controlled by using only the corresponding SubTDM.

V. Design of Controllable Full-/Controllable Semitendon-Driven Mechanisms

In Section IV, we discussed how a given TDM was divided into a number of SubTDMs. In contrast, in this section, we design a desired TDM by combining SubTDMs. As shown in (24), if we prepare some appropriate SubTDMs and combine them, then we can design any TDM in the lowest layer of Fig. 5 as a separable TDM. However, in this section, we focus only on the C-TDMs that contain most of the useful TDMs as robotic mechanisms. First, we describe some important concepts to design and describe the design procedure of C-TDMs. Next, we describe an additional condition for the design of CS-TDMs that are frequently used for underactuated fingers, as shown in Table V. We also extend this design method to a general drive system.

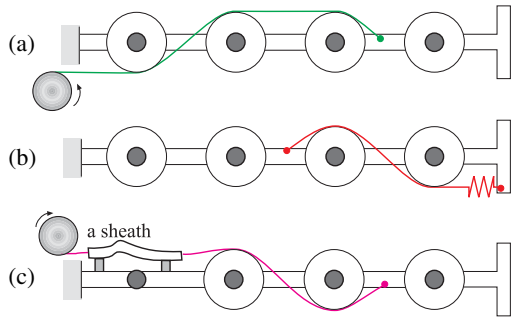

Fig. 6. Hardware properties of tendons. (a) Tendon with a large actuator. (b) Tendon with a passive element. (c) Tendon routed by a sheath.

A. Transmission Properties of Hardware

First, we consider transmission hardware. The candidates for the tendon-transmission hardware are listed as follows.

Case (a): The actuators or passive elements of tendons are attached to the basement [see Fig. 6(a)].

Case (b): The actuators or passive elements of tendons are attached to the intermediate links [see Fig. 6(b)].

Case (c): the tendons are routed by sheaths [see Fig. 6(c)].

Large actuators and passive mechanisms are usually placed at the base link because they are heavy components and decrease the payload of the mechanisms [Case (a)]. In this case, the tendons must be designed to go through a series of joints from the base link. In contrast, we can attach actuators and passive mechanisms to an intermediate link if they are adequately small [Case (b)]. Then, the tendons do not need to go through the base link, but the tendons must go through a series of joints. Sheaths are used to skip some joints and to transmit tendons to distal joints. Theoretically, sheaths can be used many times for one tendon [case (c)]. However, sheaths generate a large friction force [17]. Consequently, a design of each tendon transmission generally has only one sheath starting from the basement, which is used to skip some joints and transmit the tendons to a series of joints after the sheaths are attached to a link. Therefore, sheath-routed tendons tend to have the same series transmission property as in case (b).

To guarantee the series transmission properties of the tendons, we introduce the following definition:

Definition 5.1 [Series transmission matrix (STM)]:

1) If any element between any nonzero elements in a row is also nonzero, then the row has the series transmission property. If all rows of the matrix possess this property, then the matrix is an STM.
2) If a matrix is an STM and any column vector between any two nonzero column vectors is also a nonzero vector, then the matrix is a column series transmission matrix (CSTM).
3) If all elements of the first column vector of a CSTM are nonzero, then the matrix is a triangular series transmission matrix (TSTM).

Example 5.1: Consider the following matrices:

$$\boldsymbol{J}_1 = \begin{bmatrix} 1 & 1 & 0 & 0 & 0 \\ 0 & 0 & 0 & 1 & -1 \end{bmatrix}, \quad \boldsymbol{J}_2 = \begin{bmatrix} 1 & 1 & 0 & 0 \\ 0 & -1 & 1 & 0 \\ -1 & 1 & 1 & 0 \end{bmatrix}$$

$$\boldsymbol{J}_3 = \begin{bmatrix} 1 & 1 & 0 & 0 \\ 1 & -1 & 1 & 0 \\ -1 & 1 & 1 & 0 \end{bmatrix}, \text{ and } \boldsymbol{J}_4 = \begin{bmatrix} 1 & 1 & 0 & 1 \\ -1 & 1 & 1 & 0 \end{bmatrix}. \tag{30}$$

$\boldsymbol{J}_1$ is an STM but is not a CSTM, because the third column vector is zero. $\boldsymbol{J}_2$ is a CSTM but not a TSTM because the (2, 1) element is zero. $\boldsymbol{J}_3$ is a TSTM. $\boldsymbol{J}_4$ is not an STM because the first row vector does not satisfy the series transmission property.

In general, a TSTM is required for an actuated SubTDM, as shown in Fig. 6(a). In contrast, a CSTM is required for passive and sheathed SubTDMs, as shown in Fig. 6(b) and (c).

B. Selection of the Transmission Matrix $\bar{\boldsymbol{T}}_k$

In this section, we clarify two properties to design C-TDMs as separable TDMs.

1) Rank Condition of $\boldsymbol{T}$: By substituting (27) into (24), a Jacobian of a separable TDM is rewritten as follows:

$$\boldsymbol{J}_j = \boldsymbol{P}\boldsymbol{W}\boldsymbol{T} = \begin{bmatrix} \bar{\boldsymbol{P}}_1\bar{\boldsymbol{W}}_1 & \boldsymbol{0} & \cdots & \boldsymbol{0} \\ \boldsymbol{0} & \bar{\boldsymbol{P}}_2\bar{\boldsymbol{W}}_2 & \cdots & \boldsymbol{0} \\ \vdots & \vdots & \ddots & \vdots \\ \boldsymbol{0} & \boldsymbol{0} & \cdots & \bar{\boldsymbol{P}}_s\bar{\boldsymbol{W}}_s \end{bmatrix} \begin{bmatrix} \bar{\boldsymbol{T}}_1 \\ \bar{\boldsymbol{T}}_2 \\ \vdots \\ \bar{\boldsymbol{T}}_s \end{bmatrix}. \tag{31}$$

We can design $\bar{\boldsymbol{P}}_k\bar{\boldsymbol{W}}_k \in \mathbb{R}^{n_k \times \lambda_k}\,(k = 1, 2, \ldots, s)$ to be a column-full-rank matrix. Then, from (25) and (31), a separable TDM satisfies the condition

$$\text{rank } \boldsymbol{J}_j = \text{rank } \boldsymbol{T} = N \leq \sum_{k=1}^{s} \text{rank } \bar{\boldsymbol{T}}_k. \tag{32}$$

Therefore, we must design $\bar{\boldsymbol{T}}_k$ of SubTDMs to satisfy (32).

2) $\bar{\boldsymbol{T}}_k$ and Hardware: As discussed in Section V-A, we choose the hardware for SubTDMs to determine a series transmission property of $\boldsymbol{J}_{jk}$. $\boldsymbol{J}_{jk}$ preserves this property of $\bar{\boldsymbol{T}}_k$ after multiplication in (27) if we appropriately select $\bar{\boldsymbol{W}}_k$. We will discuss the selection of $\bar{\boldsymbol{W}}_k$ in Section V-C. Therefore, the sufficient condition is that $\bar{\boldsymbol{T}}_k$ has the same series transmission property with the desired Jacobian $\boldsymbol{J}_{jk}$ of the corresponding SubTDM.

C. Selection of a Canonical Tendon Jacobian matrix $\bar{\boldsymbol{W}}_k$

A tendon Jacobian $\boldsymbol{J}_j$ has the following property:

*Theorem 5.2 [Canonical form of tendon Jacobian [20]]:*The Jacobian matrix $\boldsymbol{J}_j$ of TDMs can be transformed into the following canonical form using Theorem III.1:

$$\boldsymbol{J}_j \rightarrow \bar{\boldsymbol{W}} = \begin{bmatrix} \boldsymbol{I}_N \\ -\boldsymbol{A}^{\mathrm{T}} \end{bmatrix} \tag{33}$$

where there exists $\boldsymbol{v} > \boldsymbol{0}$ such that $\boldsymbol{A}\boldsymbol{v} > \boldsymbol{0}$. Hereafter, $\bar{\boldsymbol{W}}$ is called a canonical tendon Jacobian. The above theorem was originally derived for CF-TDMs, but it can be applied to the tendon Jacobian $\boldsymbol{J}_{jk}$ of SubTDMs transformed into $\bar{\boldsymbol{W}}_k$.

We must consider two things to design $\bar{\boldsymbol{W}}_k$; one is the number of tendons. Generally, an N-DOF TDM requires $N + \alpha$ tendons to drive all the joints independently, where α is a natural number. $2N$ and $N + 1$ tendons are frequently used to create a decoupled transmission and a minimal drive system, respectively. We extend this discussion for the λ_k-DOF SubTDMs and choose three canonical tendon Jacobian matrices as follows:

For $L_k = 2\lambda_k$

$$\bar{\boldsymbol{W}}_k = \begin{bmatrix} \boldsymbol{I}_{\lambda_k} \\ -\boldsymbol{I}_{\lambda_k} \end{bmatrix}. \tag{34}$$

For $L_k = \lambda_k + 1$

$$\bar{\boldsymbol{W}}_k = \begin{bmatrix} \boldsymbol{I}_{\lambda_k} \\ -\boldsymbol{a}_k^{\mathrm{T}} \end{bmatrix} \tag{35}$$

where all the elements of $\boldsymbol{a}_k$ are positive real numbers.

For $L_k = \lambda_k + \alpha_k$

$$\bar{\boldsymbol{W}}_k = \begin{bmatrix} \boldsymbol{I}_{\lambda_k} \\ -\boldsymbol{A}_k^{\mathrm{T}} \end{bmatrix} \tag{36}$$

where $\boldsymbol{A}_k$ satisfies such that $\boldsymbol{A}_k\boldsymbol{v} > \boldsymbol{0}$ for a given $\boldsymbol{v} > \boldsymbol{0}$.

The other consideration is preserving the series transmission property when calculating (27). $\bar{\boldsymbol{P}}_k$ is the positive diagonal matrix and does not change the series transmission property. Therefore, the problem is how to design $\bar{\boldsymbol{W}}_k$ to preserve the series transmission property of $\bar{\boldsymbol{T}}_k$. Then, we can use the following proposition:

Proposition 5.1 [Preservation of the series transmission property]:

1) $\boldsymbol{J}_{jk}$ calculated from (27) always preserves the series transmission property of $\bar{\boldsymbol{T}}_k$ if $\bar{\boldsymbol{W}}_k$ is given in (34).
2) $\boldsymbol{J}_{jk}$ calculated from (27) preserves the series transmission property of $\bar{\boldsymbol{T}}_k$ with probability one if $\boldsymbol{a}_k$ of $\bar{\boldsymbol{W}}_k$ in (35) is a randomly selected positive number.
3) $\boldsymbol{J}_{jk}$ calculated from (27) preserves the series transmission property of $\bar{\boldsymbol{T}}_k$ with probability one if $\boldsymbol{A}_k$ of $\bar{\boldsymbol{W}}_k$ in (36) is randomly selected under the condition that $\boldsymbol{A}_k\boldsymbol{v} > \boldsymbol{0}$ for a given $\boldsymbol{v} > \boldsymbol{0}$.

The proof will be described in the Appendix C.

D. Design Procedure of Controllable Tendon-Driven Mechanisms

Design parameters for C-TDMs are given as follows:

1) Division s of C-TDMs;
2) The transmission matrix $\bar{\boldsymbol{T}}_k$;
3) The canonical tendon Jacobian $\bar{\boldsymbol{W}}_k$ from the number of tendons L_k;
4) The matrix $\bar{\boldsymbol{P}}_k$ to adjust the pulley radii.

A C-TDM can be designed as a separable TDM to combine the tendon Jacobians $\boldsymbol{J}_{jk}, (k = 1, 2, \ldots, s)$ of the SubTDMs as (24). The design procedure is given as follows:

1) Determine $\bar{\boldsymbol{T}}_k$ to satisfy (32) and the desired series transmission property (CSTM or TSTM).
2) Determine L_k from $2\lambda_k, \lambda_k + 1$, or $\lambda_k + \alpha_k$ and design the corresponding canonical tendon Jacobians $\bar{\boldsymbol{W}}_k$. When $L_k = \lambda_k + 1$ and $\lambda_k + \alpha_k$, we appropriately determine $\boldsymbol{a}_k$ and $\boldsymbol{A}_k$, respectively, in $\bar{\boldsymbol{W}}_k$.
3) Multiply $\bar{\boldsymbol{W}}_k$ by $\bar{\boldsymbol{T}}_k$. When $L_k = \lambda_k + 1$ or $\lambda_k + \alpha_k$, check whether the series transmission property of $\bar{\boldsymbol{W}}_k\bar{\boldsymbol{T}}_k$ is preserved. If not, repeat the previous procedure.
4) Determine the diagonal elements of $\bar{\boldsymbol{P}}_k$ to adjust the size of the pulley radii in $\boldsymbol{J}_{jk}$.

Example 5.2: Design 3 two-DOF C-TDMs that have all the actuators and elastic elements in the basement. Therefore, $\bar{\boldsymbol{T}}_k$ must be a TSTM, and we define $\bar{\boldsymbol{T}}_k$ as follows:

$$\bar{\boldsymbol{T}}_k = \begin{bmatrix} -1 & 0 \\ 1 & 1 \end{bmatrix}. \tag{37}$$

Here, we generate three $\bar{\boldsymbol{W}}_k$, $(i = 1, 2, 3)$, which correspond to $L_k = 2\lambda_k$, $\lambda_k + 1$, and $\lambda_k + 2$, respectively, as follows:

$$\bar{\boldsymbol{W}}_1 = \begin{bmatrix} \boldsymbol{I}_2 \\ -\boldsymbol{I}_2 \end{bmatrix}, \bar{\boldsymbol{W}}_2 = \begin{bmatrix} 1 & 0 \\ 0 & 1 \\ -2 & -1 \end{bmatrix}, \bar{\boldsymbol{W}}_3 = \begin{bmatrix} 1 & 0 \\ 0 & 1 \\ -2 & -1 \\ 0 & -1 \end{bmatrix}.$$

$\bar{\boldsymbol{P}}_k (k = 1, 2, 3)$ is the identity matrix with the corresponding dimension. Then, $\boldsymbol{J}_{jk}$ in (27) is given as follows:

$$\boldsymbol{J}_{j1} = \begin{bmatrix} -1 & 0 \\ 1 & 1 \\ 1 & 0 \\ -1 & -1 \end{bmatrix}, \boldsymbol{J}_{j2} = \begin{bmatrix} -1 & 0 \\ 1 & 1 \\ 1 & -1 \end{bmatrix}, \boldsymbol{J}_{j3} = \begin{bmatrix} -1 & 0 \\ 1 & 1 \\ 1 & -1 \\ -1 & -1 \end{bmatrix}.$$

$\boldsymbol{J}_{jk}$ $(k = 1, 2, 3)$ corresponds to the $\boldsymbol{J}_j$ of (CS-2), (CF-2), and (CF-4), respectively, with the exception of the row vector orders.

E. Special Property of Controllable Semi-tendon-Driven Mechanism

CS-TDMs have fewer independent actuators than numbers of joints. Thus, possible joint configuration of CS-TDMs are determined by the static balance (15) that depends on the stiffness of the passive tendons. However, it is generally difficult to identify the tendon stiffness precisely, and consequently, it is difficult to estimate the joint configuration precisely.

On the other hand, it is possible to decouple the possible joint configuration from the static balance of the passive tendons if we appropriately design the tendon Jacobian. In addition, the obtained CS-TDM efficiently changes the joint configuration in terms of the actuation power. The key idea is to design a CS-TDM as a decoupled TDM by combining an UF-TDM and an UP-TDM. Then, we have

$$\boldsymbol{l}_1 = \boldsymbol{J}_{j1}\boldsymbol{q} + \boldsymbol{g}_1(\boldsymbol{\theta}, \boldsymbol{l}_0) = \bar{\boldsymbol{P}}_1\bar{\boldsymbol{W}}_1\bar{\boldsymbol{T}}_1\boldsymbol{q}_1 + \boldsymbol{g}_1(\boldsymbol{\theta}, \boldsymbol{l}_{01}) \tag{38}$$

$$\boldsymbol{l}_2 = \boldsymbol{J}_{j2}\boldsymbol{q} + \boldsymbol{l}_{02} = \bar{\boldsymbol{P}}_2\bar{\boldsymbol{W}}_2\bar{\boldsymbol{T}}_2\boldsymbol{q}_2 + \boldsymbol{l}_{02} \tag{39}$$

where the rank condition (32) is satisfied. Equations (38) and (39) are an UF-TDM and an UP-TDM, respectively. Note that (39) expresses the joint constraint when no external force affects the CS-TDM. Thus, the joint constraint is given as follows:

$$\bar{\boldsymbol{T}}_2\boldsymbol{q} - \bar{\boldsymbol{q}}_{2\mathrm{init}}(\boldsymbol{l}_{02}) = \boldsymbol{0} \tag{40}$$

where $\bar{\boldsymbol{q}}_{2\mathrm{init}}$ is constant and the initial angle of $\bar{\boldsymbol{q}}_2$ determined by the initial tendon stretch $\boldsymbol{l}_{02}$. Using (31), (26) is rewritten as follows:

$$\text{rank } \boldsymbol{T} = \text{rank } \bar{\boldsymbol{T}}_1 + \text{rank } \bar{\boldsymbol{T}}_2 = N \tag{41}$$

where $\bar{\boldsymbol{T}}_1$ and $\bar{\boldsymbol{T}}_2$ are the STMs of an UF-TDM and an UP-TDM, respectively. This means that $\boldsymbol{T}$ must be a $N \times N$ nonsingular matrix.

Therefore, CS-TDMs are designed as a decoupled TDM and design procedure 1 listed in Section V-D is accommodated as follows:

Determine $\bar{\boldsymbol{T}}_2$ satisfying the joint constraint (40), and select a desired series transmission property;
Determine $\bar{\boldsymbol{T}}_1$ satisfying (41) and select a desired series transmission property.

F. Extension of the General Drive System

As shown in Table V, robotic fingers have frequently been designed with a combination of tendons, elastic joints, and complex linkages with elastic elements, i.e., as CS-mechanisms. The primary difference between TDMs and conventional drive systems is that a tendon produces only unilateral force, while a conventional actuator or spring produces bilateral force. $\bar{\boldsymbol{W}}_k$ and $\bar{\boldsymbol{P}}_k$ are used to transform the unilateral transmission to a bilateral one and to determine the pulley radius at the joints. In addition, bilateral transmissions are generally separable and can neglect the series transmission property. Thus, the Jacobian of each transmission is given as follows:

$$\boldsymbol{J}_{jk} = \begin{cases} \bar{\boldsymbol{P}}_k\bar{\boldsymbol{W}}_k\bar{\boldsymbol{T}}_k, & \text{if a TDM,} \\ \bar{\boldsymbol{T}}_k, & \text{if a bilateral drive system.} \end{cases} \tag{42}$$

Therefore, we only need to consider design procedure 1 in Section V-D when we design a bilateral system instead of a SubTDM.

VI. Implementation

In this section, to validate the proposed method, we design two types of CS-TDMs: three-joint adaptive grasping mechanisms and an index finger robot.

A. Three-Joint Adaptive Grasping Mechanisms

A three-joint adaptive grasping mechanism was designed using three different methods. It has a single driving DOF under two constraints, $q_1 = q_2 = q_3$.

First, we examined this finger designed using a simple torsion spring mechanism and a pair of the tendons, as shown in Fig. 7(a) [35], [37], [38]. A torsion spring is attached at each joint. Two active tendons, which span from the bottom to the end, are pulled to bend or stretch all the joints simultaneously.

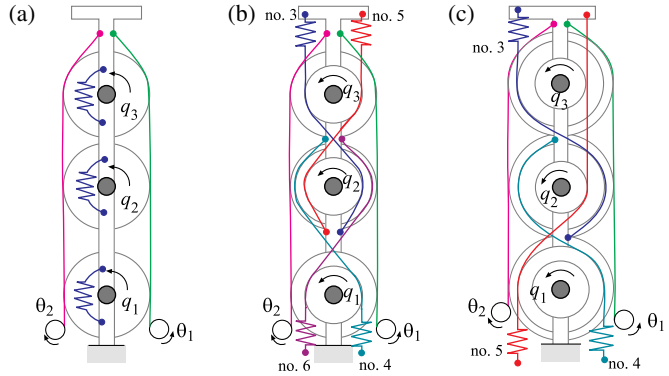

Fig. 7. Design of three DOF fingers to bend all the joint angles equally. (a) Torsion spring case. (b) Four passive tendon case. (c) Three passive tendon case.

The transmission matrix $\boldsymbol{T}$ is given as follows:

$$\boldsymbol{T} = \begin{bmatrix} \bar{\boldsymbol{T}}_1 \\ \bar{\boldsymbol{T}}_2 \end{bmatrix} = \begin{bmatrix} 1 & -1 & 0 \\ 1 & 0 & 0 \\ 0 & 1 & 0 \\ 0 & 0 & 1 \end{bmatrix} \tag{43}$$

where $\bar{\boldsymbol{T}}_1$ is the STM of the UF-TDM and $\bar{\boldsymbol{T}}_2$ is the STM of the torsion spring. This $\bar{\boldsymbol{T}}_k$ clearly satisfies the condition (32). Because the torsion springs are bilateral systems, we only design the tendon Jacobian of the UF-TDM, as shown in Section V-F. Let $\bar{\boldsymbol{P}}_1$ be the identity matrix, for simplicity, and $\bar{\boldsymbol{W}}_1$ is the canonical tendon Jacobian for $L_k = 2\lambda_k$ as follows:

$$\bar{\boldsymbol{W}}_1 = \begin{bmatrix} 1 \\ -1 \end{bmatrix}. \tag{44}$$

Then, the tendon kinematics for the active tendons is given as follows:

$$\boldsymbol{l}_1 = \boldsymbol{J}_{j1}\boldsymbol{q} + \boldsymbol{R}_a\boldsymbol{\theta} \tag{45}$$

$$\text{where } \boldsymbol{J}_{j1} = \bar{\boldsymbol{P}}_1\bar{\boldsymbol{W}}_1\bar{\boldsymbol{T}}_1 = \begin{bmatrix} 1 & 1 & 1 \\ -1 & -1 & -1 \end{bmatrix}. \tag{46}$$

From (43), the grasping mechanism is separable but is not decoupled. Thus, the tensile forces depend on the current joint angle. Let k_s be the spring coefficient on the joints. Then, the joint torque generated by the tendons and the springs at an equilibrium point is given as follows:

$$\boldsymbol{\tau} = -\boldsymbol{J}_{j1}^{\mathrm{T}} \begin{bmatrix} f_{t1} \\ f_{t2} \end{bmatrix} - k_s\boldsymbol{q} = (f_{t2} - f_{t1}) \begin{bmatrix} 1 \\ 1 \\ 1 \end{bmatrix} - k_s \begin{bmatrix} q_1 \\ q_2 \\ q_3 \end{bmatrix} = \boldsymbol{0}. \tag{47}$$

Then, all the joints satisfy that

$$q_i = \frac{f_{t2} - f_{t1}}{k_s} = \alpha \text{ for } i = 1, 2, 3 \tag{48}$$

where α is a constant. Each torsion spring torque equals $-k_s\alpha$; thus, the tensile forces are given as follows:

$$\begin{bmatrix} f_{t1} \\ f_{t2} \end{bmatrix} = -\frac{k\alpha}{2} \begin{bmatrix} 1 \\ -1 \end{bmatrix} + f_b \begin{bmatrix} 1 \\ 1 \end{bmatrix}. \tag{49}$$

The more the joints bend, the greater the tensile forces become. Therefore, the torsion spring coefficients must be small to maintain low tensile forces. In contrast, when some tasks require high joint stiffness, the actuators require large tensile forces for a small joint rotation. Note that this mechanism requires all the joints to be exactly the same stiffness k_s . Otherwise, the joint motion can no longer satisfy the constraint $q_1 = q_2 = q_3$.

Next, we designed the same mechanism using the proposed method, as described in Section V-D and V-E. In this case, the constraints are given as $q_1 = q_2 = q_3$, and we allow passive elements to be placed on the link. Therefore, the matrix $\bar{\boldsymbol{T}}_2$ must be a CSTM. Then, the constraints are rewritten as follows:

$$\begin{bmatrix} q_2 - q_3 \\ q_1 - q_2 \end{bmatrix} = \bar{\boldsymbol{T}}_2\boldsymbol{q} = \begin{bmatrix} 0 & 1 & -1 \\ 1 & -1 & 0 \end{bmatrix} \boldsymbol{q} = \boldsymbol{0}. \tag{50}$$

We use $\bar{\boldsymbol{T}}_1$ in (43) as the STM of the UF-TDM. Therefore, $\bar{\boldsymbol{T}}_i (i = 1, 2)$ satisfies the condition (41). Each SubTDM is constructed using $2\lambda_k$ tendons. Then, $\bar{\boldsymbol{W}}_1$ is given in (44) and $\bar{\boldsymbol{W}}_2$ is given as follows:

$$\bar{\boldsymbol{W}}_2 = \begin{bmatrix} \boldsymbol{I}_2 \\ -\boldsymbol{I}_2 \end{bmatrix}. \tag{51}$$

$\boldsymbol{P}_k (k = 1, 2)$ is assumed to be the identity matrix. Therefore, the TDM is decoupled, as shown in (38) and (39), where the tendon Jacobian of the UF-TDM is given in (46), and that of the UP-TDM is given as follows:

$$\boldsymbol{J}_{j2} = \bar{\boldsymbol{P}}_2\bar{\boldsymbol{W}}_2\bar{\boldsymbol{T}}_2 = \begin{bmatrix} 0 & 1 & -1 \\ 1 & -1 & 0 \\ 0 & -1 & 1 \\ -1 & 1 & 0 \end{bmatrix}. \tag{52}$$

The obtained mechanism is a CS-TDM, as shown in Fig. 7(b), which is a combination of the mechanisms in Fig. 3 (CF-1) and Fig. 4 (UF-4).

Let k_s be the spring coefficient of the tendons in the UP-TDM, each joint angle q_i be α and (f_{t1}, f_{t2}) be the tensile force of the UF-TDM. Then, the static joint torque is given as follows:

$$\boldsymbol{\tau} = -\boldsymbol{J}_{j1}^{\mathrm{T}} \begin{bmatrix} f_{t1} \\ f_{t2} \end{bmatrix} - k_s\boldsymbol{J}_{j2}^{\mathrm{T}}\boldsymbol{J}_{j2} \begin{bmatrix} 1 \\ 1 \\ 1 \end{bmatrix} \alpha = (f_{t2} - f_{t1}) \begin{bmatrix} 1 \\ 1 \\ 1 \end{bmatrix} = \boldsymbol{0}. \tag{53}$$

This means that the tensile forces do not depend on the joint configuration and are in equilibrium with the bias force $\boldsymbol{f}_b$ at any configuration. The stiffness can be determined as a task requires. Therefore, the mechanism in Fig. 7(b) is more efficient than that in Fig. 7(a). This mechanism has four springs, the number of which is greater than that used in Fig. 7(a). This mechanism can easily reduce the number of the passive tendons to three, similar to the mechanism in Fig. 7(a), by introducing $\lambda_k + 1$ tendons to the UP-TDM. In this case

$$\bar{\boldsymbol{W}}_2 = \begin{bmatrix} 1 & 0 \\ 0 & 1 \\ -0.5 & -1 \end{bmatrix}. \tag{54}$$

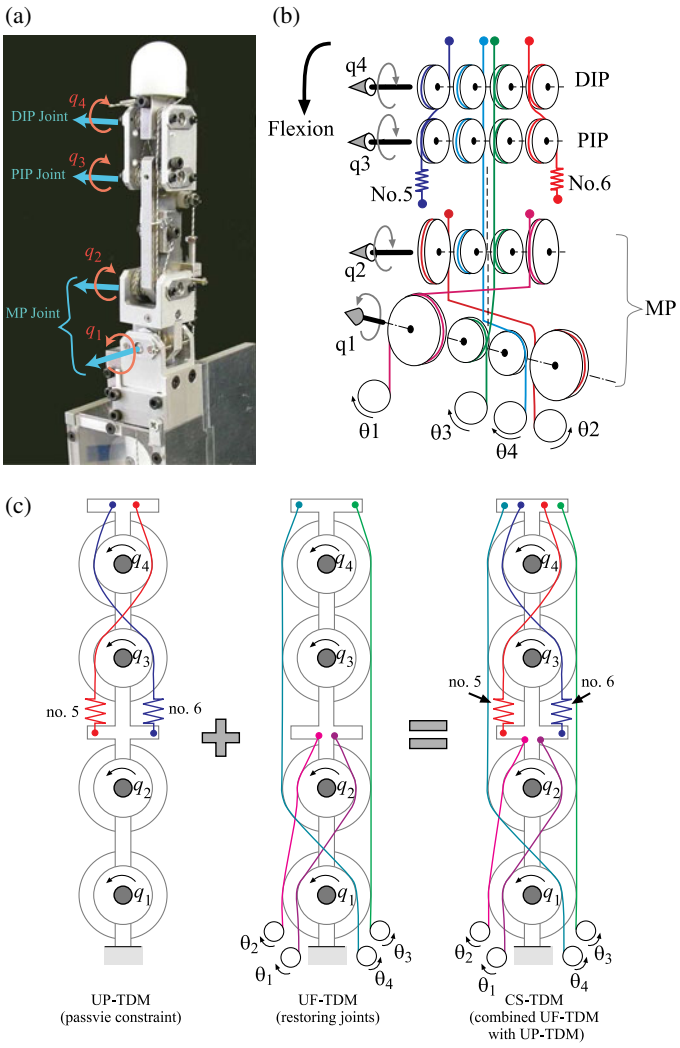

Fig. 8. Tendon-driven index finger. (a) Photo of the completed index finger. (b) Entire tendon-routing. (c) Design process of the tendon routing.

Then, the tendon Jacobian is given as follows:

$$\boldsymbol{J}_{j2} = \bar{\boldsymbol{P}}_2 \bar{\boldsymbol{W}}_2 \bar{\boldsymbol{T}}_2 = \begin{bmatrix} 0 & 1 & -1 \\ 1 & -1 & 0 \\ -1 & 0.5 & 0.5 \end{bmatrix} \tag{55}$$

which corresponds to the CS-TDM in Fig. 7(c). This mechanism works as the CS-TDM in Fig. 7(b), and it also does not use any torque to maintain a configuration.

B. Index Finger Robot

The human index finger is generally modeled as a four-joint mechanism, where the metacarpal phalangeal (MP) joint has two orthogonal joint axes and the PIP and DIP joints have one joint axis, as shown in Fig. 8. The PIP and DIP joints move together and are useful in absorbing external forces when the fingertip makes contact with the environment, as shown in Fig. 9 [7]. Therefore, the driving DOF of this mechanism is three. Let $\boldsymbol{q} = (q_1, q_2, q_3, q_4)$ be the joint angle. The constraint between the DIP and PIP joints is given as $q_3 - q_4 = 0$, and it is realized

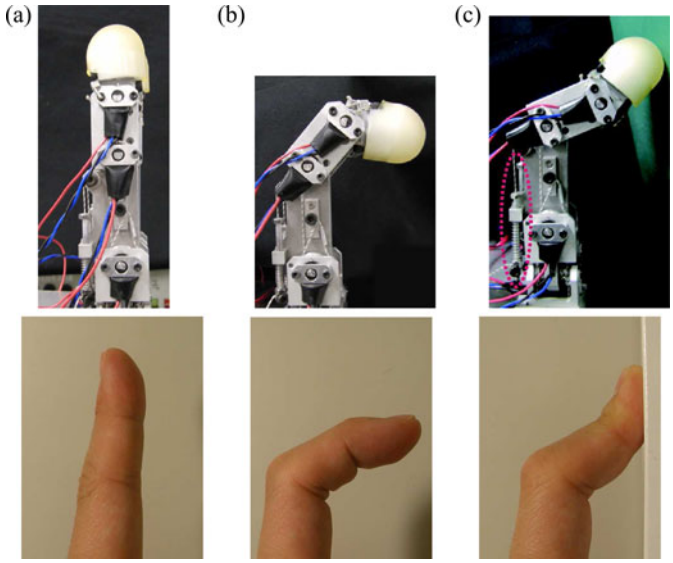

Fig. 9. Constrained motion of the DIP and DIP joints [7]. (a) Initial posture. (b) Bending posture. (c) Contact posture. The elastic elements surrounded by the red dashed line absorb the external force.

using pulley-routed passive tendons. Therefore, the constraint motion is described using the CSTM as follows:

$$q_3 - q_4 = \bar{\boldsymbol{T}}_2 \boldsymbol{q} = 0, \text{ where } \bar{\boldsymbol{T}}_2 = [0 \quad 0 \quad 1 \quad -1]. \tag{56}$$

The remaining index finger DOF must move independently. We choose three decoupling variables for the active part as follows:

$$\bar{\boldsymbol{q}}_1 = \begin{bmatrix} -q_1 + q_2 \\ -q_1 - q_2 \\ \sum_{i=1}^{4} q_i \end{bmatrix} = \bar{\boldsymbol{T}}_1 \boldsymbol{q} = \begin{bmatrix} -1 & 1 & 0 & 0 \\ -1 & -1 & 0 & 0 \\ 1 & 1 & 1 & 1 \end{bmatrix} \boldsymbol{q} \tag{57}$$

which is a TSTM and is independently equivalent to the control q_1, q_2, and q_3 . These $\bar{\boldsymbol{T}}_i, (i = 1, 2)$ satisfy the condition (41). Therefore, we can realize the tendon routes using only the pulleys and actuators mounted on the base.

Let $\bar{\boldsymbol{P}}_1 = \text{diag.}(R, R, r, r)$ and $\bar{\boldsymbol{P}}_2 = \text{diag.}(r, r)$, where $r = 4.5 \times 10^{-3}$ m and $R = 7.0 \times 10^{-3}$ m. The active and passive parts of the canonical tendon Jacobians are designed using the $\lambda_k + 1$ and $2\lambda_k$ tendons as follows:

$$\bar{\boldsymbol{W}}_1 = \begin{bmatrix} 1 & 0 & 0 \\ 0 & 1 & 0 \\ 0 & 0 & 1 \\ -1 & -1 & -1 \end{bmatrix}, \text{ and } \bar{\boldsymbol{W}}_2 = \begin{bmatrix} 1 \\ -1 \end{bmatrix}. \tag{58}$$

Then, the TDM is decoupled, as shown in (38) and (39), and the tendon Jacobians are given as follows:

$$\boldsymbol{J}_{j1} = \bar{\boldsymbol{P}}_1 \bar{\boldsymbol{W}}_1 \bar{\boldsymbol{T}}_1 = \begin{bmatrix} -R & R & 0 & 0 \\ -R & -R & 0 & 0 \\ r & r & r & r \\ r & -r & -r & -r \end{bmatrix} \tag{59}$$

$$\boldsymbol{J}_{j2} = \bar{\boldsymbol{P}}_2 \bar{\boldsymbol{W}}_2 \bar{\boldsymbol{T}}_2 = \begin{bmatrix} 0 & 0 & r & -r \\ 0 & 0 & -r & r \end{bmatrix}. \tag{60}$$

The bias force is given as follows:

$$\boldsymbol{f}_b = \begin{bmatrix} R & 0 \\ R & 0 \\ r & 0 \\ r & 0 \\ \hline 0 & 1 \\ 0 & 1 \end{bmatrix} \begin{bmatrix} \xi_1 \\ \xi_2 \end{bmatrix}.$$

Fig. 8 shows the completed index finger robot. Here, we focus on the PIP and DIP joints, as shown in Fig. 9(b). In free motion, the joints move together as a result of the cross-coupling of passive tendons. In the case where the fingertip is constrained by the environment, the joints move independently, utilizing the external force, and the robotic finger's passive tendon mechanism absorbs the external force. The connected motion has been used in many robotic hands [9], [31], [32], [39], [40]. However, the couplings were rigid because the fingertip could not passively react to the external force [9], [31], [32], [39], or a torsion spring was installed only on the DIP joint, where only the DIP joint passively reacts to the external force at the fingertip [40]. As shown in Fig. 9(c), the human PIP joint moves conversely to the DIP joint during the contact, and this feature naturally appears in the elastic cross-coupling connection between the IP joints of this mechanism [7], [41].

Variables q_1 and q_2 in (57) are coupled in the above design, but one might prefer these variables to be decoupled. Then, the decoupling variable $\bar{\boldsymbol{q}}_1^{\mathrm{de}}$ is simpler than (57) as follows:

$$\bar{\boldsymbol{q}}_1^{\mathrm{de}} = \begin{bmatrix} q_1 \\ q_2 \\ \sum_{i=2}^{4} q_i \end{bmatrix} = \bar{\boldsymbol{T}}_1^{\mathrm{de}} \boldsymbol{q} = \begin{bmatrix} 1 & 0 & 0 & 0 \\ 0 & 1 & 0 & 0 \\ 0 & 1 & 1 & 1 \end{bmatrix} \boldsymbol{q}. \tag{61}$$

$\bar{\boldsymbol{T}}_1^{\mathrm{de}}$ is a CSTM. Then, the corresponding tendon Jacobian matrix is given as follows:

$$\boldsymbol{J}_{j1} = \bar{\boldsymbol{P}}_1 \bar{\boldsymbol{W}}_1 \bar{\boldsymbol{T}}_1^{\mathrm{de}} = \begin{bmatrix} R & 0 & 0 & 0 \\ 0 & R & 0 & 0 \\ 0 & r & r & r \\ -r & -2r & -r & -r \end{bmatrix}. \tag{62}$$

$\boldsymbol{J}_{j1}$ is a CSTM, and when the actuators are attached at the basement, a sheath is required to transmit to the second and the third tendons, because the tendons skip the first joint.

VII. Conclusion

In this paper, we classified TDMs with active and passive tendons using algebraic analyses and proposed a design method for C-TDMs, which are equivalent to conventional drive mechanisms, and CS-TDMs with the kinematic constraints of passive tendons. This design method is applicable only to pulley-routed TDMs, although pulley-routed TDMs have many applications. In our analyses, the pulley-routed TDMs are classified into six TDMs (CF/CS/CP/UF/US/UP-TDMs) from two perspectives: controllability and driving DOF. This classification revealed the difference between two underactuated TDMs: CS-TDMs and UF-TDMs. This difference was not previously recognized and is useful in the design of grasping mechanisms.

We also showed that the TDMs are decomposed into SubTDMs based on the bias force analysis. We proposed a method for designing a C-TDM by combining SubTDMs. In particular, we proposed a method for designing efficient CS-TDMs with two decoupled SubTDMs. This design method can be applied to TDMs combined with bilateral driving elements, such as motors and torsion springs, which are often used in robotic systems.

Based on this design method, we designed three-joint adaptive gripper mechanisms and demonstrated that two of these adaptive grippers use less driving force than the other, which is the conventional adaptive gripper mechanism to maintain an arbitrary configuration. We also demonstrated the design of an index finger robot with two special interphalangeal joints, which move together in free space and coordinate to absorb external forces when the fingertip is constrained, to mimic the features of the human index finger.

The designed joint constraints on CS-TDMs can be maintained by using UP-TDMs when the effect of the gravitational force is relatively smaller than the elastic force in UP-TDMs, as shown in the index finger robot in Fig. 8. In this example, we roughly determined the stiffness of the tendons. However, generally speaking, it is important to determine the optimal stiffness based on the gravitational force and the operations that robots perform.

The proposed design method simplifies the design of the wire-routing of TDMs compared with conventional methods. In contrast, we did not treat some problems that were considered in conventional methods, such as torque optimization [18], the constraints between the fingers [8], [42], and the maximal active tensions of the tendons to determine the grasp qualities of a hand [43], [44].

In future studies, we will expand the proposed method to include optimizeing the stiffness and driving force and apply these methods to more general mechanisms, such as suspended TDMs or a hand mechanism with constraints between the fingers.

Appendix A
Proof of Proposition III.1

The sufficient condition of C-TDMs is obvious, thus only the necessary condition of C-TDMs is considered. We assume that rank $\boldsymbol{J}_j$ of C-TDMs is smaller than N. It follows that there exists a nonzero vector $\boldsymbol{v}$ such that

$$\boldsymbol{J}_j \boldsymbol{v} = \boldsymbol{0}. \tag{63}$$

From (3), the recovery torque by the infinitesimal joint displacement $\Delta\boldsymbol{q} = \boldsymbol{q} - \boldsymbol{q}_0$ is given as follows:

$$\boldsymbol{\tau} = -\boldsymbol{J}_j^{\mathrm{T}} \boldsymbol{K}_t \boldsymbol{J}_j \Delta\boldsymbol{q} \tag{64}$$

where $\boldsymbol{K}_t = \mathrm{diag.}(\boldsymbol{K}_a, \boldsymbol{K}_e)$. If $\Delta\boldsymbol{q} = \boldsymbol{v}$, then

$$\boldsymbol{\tau} = -\boldsymbol{J}_j^{\mathrm{T}} \boldsymbol{K}_t \boldsymbol{J}_j \boldsymbol{v} = \boldsymbol{0} \tag{65}$$

and no recovery torque is generated, and $\boldsymbol{q}_0$ is not a stable equilibrium point. Therefore, the assumption is not correct, and

the rank of $\boldsymbol{J}_j$ of the C-TDMs must be equal to N. U-TDMs do not have any stable equilibrium point, thus the rank of $\boldsymbol{J}_j$ of U-TDMs must be smaller than N.

APPENDIX B
PROOF OF PROPOSITION IV.1

We consider two sub-bias forces $\boldsymbol{f}_{b1}$ and $\boldsymbol{f}_{b2}$ such that

$$\boldsymbol{f}_{b1} = \begin{bmatrix} \bar{\boldsymbol{f}}_{b1} \\ \bar{\boldsymbol{p}}_{b1} \end{bmatrix} \text{ and } \boldsymbol{f}_{b2} = \begin{bmatrix} \boldsymbol{0} \\ \bar{\boldsymbol{f}}_{b2} \end{bmatrix} \tag{66}$$

where $\bar{\boldsymbol{f}}_{bi} > \boldsymbol{0}$ is a positive vector and $\bar{\boldsymbol{p}}_{b1}$ is a nonnegative and nonzero vector. To confirm the orthogonality of the sub-bias forces, we calculate the inner product between the sub-bias forces as follows:

$$\boldsymbol{f}_{b1}^{\mathrm{T}} \boldsymbol{f}_{b2} = \bar{\boldsymbol{p}}_{b1}^{\mathrm{T}} \bar{\boldsymbol{f}}_{b2} > 0. \tag{67}$$

Therefore, the sub-bias forces are not orthogonal. To make them orthogonal to each other, we must eliminate the nonzero elements of $\bar{\boldsymbol{p}}_{b1}$ in the same rows of $\bar{\boldsymbol{f}}_{b2}$. In the general case, to be orthogonal to each other the sub-bias force vectors $\boldsymbol{f}_{bi} (i = 1, 2, \ldots, s)$ must not possess any positive elements in the common rows, and they are given as follows:

$$\boldsymbol{f}_{b1} = \begin{bmatrix} \bar{\boldsymbol{f}}_{b1} \\ \boldsymbol{0} \\ \boldsymbol{0} \\ \vdots \\ \boldsymbol{0} \end{bmatrix}, \boldsymbol{f}_{b2} = \begin{bmatrix} \boldsymbol{0} \\ \bar{\boldsymbol{f}}_{b2} \\ \boldsymbol{0} \\ \vdots \\ \boldsymbol{0} \end{bmatrix} \cdots, \text{ and } \boldsymbol{f}_{br} = \begin{bmatrix} \boldsymbol{0} \\ \boldsymbol{0} \\ \vdots \\ \boldsymbol{0} \\ \bar{\boldsymbol{f}}_{bs} \end{bmatrix}. \tag{68}$$

Next, consider the TDM

$$\boldsymbol{l} = \begin{bmatrix} \boldsymbol{l}_1 \\ \boldsymbol{l}_2 \\ \vdots \\ \boldsymbol{l}_s \end{bmatrix} = \begin{bmatrix} \boldsymbol{J}_{j1} \\ \boldsymbol{J}_{j2} \\ \boldsymbol{J}_{j3} \\ \vdots \\ \boldsymbol{J}_{js} \end{bmatrix} \boldsymbol{q} + \begin{bmatrix} \boldsymbol{g}_1(\boldsymbol{\theta}_1, \boldsymbol{l}_{01}) \\ \boldsymbol{g}_2(\boldsymbol{\theta}_2, \boldsymbol{l}_{02}) \\ \vdots \\ \boldsymbol{g}_s(\boldsymbol{\theta}_s, \boldsymbol{l}_{0s}) \end{bmatrix} \tag{69}$$

where $\boldsymbol{\theta} = (\boldsymbol{\theta}_1, \boldsymbol{\theta}_2, \ldots, \boldsymbol{\theta}_s)$, and $\boldsymbol{l}_0 = (\boldsymbol{l}_{01}, \boldsymbol{l}_{02}, \ldots, \boldsymbol{l}_{0s})$. $\boldsymbol{l}_i (i = 1, 2, \ldots, s)$ is the tendon stretch corresponding to $\bar{\boldsymbol{f}}_{bi}$. From the definition of the sub-bias forces

$$\boldsymbol{J}_j^{\mathrm{T}} \boldsymbol{f}_{bi} = \boldsymbol{J}_{ji}^{\mathrm{T}} \bar{\boldsymbol{f}}_{bi} = \boldsymbol{0} \tag{70}$$

$\bar{\boldsymbol{f}}_{bi}$ is in the null-space of $\boldsymbol{J}_{jk}^{\mathrm{T}}$, and each TDM $\boldsymbol{l}_i (i = 1, 2, \ldots, s)$ has the bias force $\bar{\boldsymbol{f}}_{bi} > \boldsymbol{0}$. Therefore, the TDM is separable in the case that $\boldsymbol{J}_{ji} (i = 1, 2, \ldots, s)$ does not possess any common row.

APPENDIX C
PROOF OF PROPOSITION V.1

The $\lambda_k + 1$ type case will be proven. Let

$$\boldsymbol{T}_k = \begin{bmatrix} \boldsymbol{t}_1 \\ \boldsymbol{t}_2 \\ \vdots \\ \boldsymbol{t}_{\lambda_k} \end{bmatrix}. \tag{71}$$

Then,

$$\bar{\boldsymbol{W}}_k \bar{\boldsymbol{T}}_k = \begin{bmatrix} \boldsymbol{t}_1 \\ \boldsymbol{t}_2 \\ \vdots \\ \boldsymbol{t}_{\lambda_k} \\ \boldsymbol{t}_{\lambda_k+1} \end{bmatrix}, \text{ where } \boldsymbol{t}_{\lambda_k+1} = -\sum_{i=1}^{\lambda_k} a_i \boldsymbol{t}_i. \tag{72}$$

The λ_k th tendon spans from the d th joint to the e th joint, which is the most distal joint that the tendons reach because $\boldsymbol{T}_k$ is a CSTM/TSTM. Then, $t_{\lambda_k, j} \neq 0, (j = d, d+1, \ldots, e)$ and $t_{i,j} = 0, (i = 1, 2, \ldots, \lambda_k$, and $j = e+1, e+2, \ldots, \lambda_k)$. Here, consider the polynomial equation

$$f(\boldsymbol{a}_k) = \prod_{j=d}^{e} \left| \sum_{i=1}^{\lambda_k} a_{ki} t_{i,j} \right|^2. \tag{73}$$

$f(\boldsymbol{a}_k)$ is zero only if the vector $\boldsymbol{a}_k$ lies on one of $\lambda_k - 1$ dimensional hyper-planes $\mathcal{P}_j = \{\boldsymbol{a}_k | \sum_{i=1}^{\lambda_k} a_{ki} t_{i,j} = 0\}$. Thus, if we randomly choose a_{ki} from the positive real numbers, then $f(\boldsymbol{a}_k) \neq 0$ is satisfied with a probability of one. Therefore, $\boldsymbol{J}_{jk}$ is a CSTM/TSTM.

Therefore, the proposition for the case of $\lambda_k + 1$ type is proven. In the case of the $\lambda_k + \alpha$ type, we replace $\boldsymbol{t}_{\lambda_k+1} = -\sum_{i=1}^{\lambda_k} a_{ki} \boldsymbol{t}_i$ in (72) with $\boldsymbol{T}_{\lambda_k+1} = -\sum_{i=1}^{\lambda_k} \boldsymbol{a}_{ki} \boldsymbol{t}_i$, where $\boldsymbol{a}_{ki}$ is the ith column vector of $\boldsymbol{A}_k^{\mathrm{T}}$. Applying a similar argument to the proof of the $\lambda_k + 1$ type, we can show that if we randomly choose a matrix $\boldsymbol{A}_k$ from the $\alpha \times \lambda_k$ dimensional subspace $\mathcal{A}_v = \left\{ \boldsymbol{A}_k^{\mathrm{T}} | \boldsymbol{A}_k \boldsymbol{v} > \boldsymbol{0} \right\}$ for given $\boldsymbol{v} > \boldsymbol{0}$, then $\boldsymbol{J}_{jk}$ is a CSTM/TSTM with a probability of one.

The $2\lambda_k$-type is the special case of the $\lambda_k + 1$-type, and is regarded as λ_k decoupled SubTDMs with $1 + 1$ tendons. Therefore, the $2\lambda_k$-type is always a CSTM/TSTM.

REFERENCES

[1] M. C. Carrozza, "The SPRING hand: Development of a self-adaptive prosthesis for restoring natural grasping," *Auton. Robots*, vol. 16, pp. 125–141, 2004.

[2] J. Zhao, L. Jiang, S. Shi, H. Cai, H. Liu, and G. Hirzinger, "A five-fingered underactuated prosthetic hand system," in *Proc. IEEE Conf. Mechatronics Autom.*, Luoyang, China, Jun. 2006, pp. 1453–1458.

[3] S. Hirose and Y. Umetani, "The development of soft gripper for the versatile robot hand," *Mech. Mach. Theory*, vol. 13, pp. 351–359, 1978.

[4] G. Figliolini and M. Ceccarelli, "A novel articulated mechanism mimicking the motion of index finger," *Robotica*, vol. 20, pp. 13–22, 2002.

[5] G. Figliolini and P. Rea, "Overall design of Ca.U.M.Ha. robotic hand for harvesting horticulture products," *Robotica*, vol. 24, pp. 329–331, 2005.

[6] M. Kaneko, R. Higashimori, M. Takenaka, A. Namiki, and M. Ishikawa, "The 100 G capturing robot—too fast to see," *IEEE/ASME Trans. Mechatronics*, vol. 8, no. 1, pp. 37–44, Mar. 2003.

[7] R. Ozawa, K. Hashirii, and H. Kobayashi, "Design and control of underactuated tendon-driven mechanisms," in *Proc. IEEE Conf. Robot. Autom.*, Kobe, Japan, May 2009, pp. 1522–1527.
[8] L. Birglen, T. Laliberte, and C. Gosselin, *Underactuated Robotic Hands*, (Springer tracts in advance robotics Series), Berlin, Germany Springer-Verlag, 2008, vol. 40.
[9] H. Liu, P. Meusel, N. Seitz, B. Willberg, G. Hirzinger, M. H. Jin, Y. W. Liu, R. Wei, and Z. W. Xie, "The modular multisensory DLR-HIT-hand," *Mech. Mach. Theory*, vol. 42, pp. 612–625, 2007.
[10] K. Koganezawa and Y. Ishizuka, "Novel mechanism of artificial fingers," presented at the *IEEE Conf. Advanced Intell. Mechatronics*, Zurich, Switzerland, Sep. 2007.
[11] W. T. Townsend, "The effect of transmission design on force-controlled manipulator performance," Ph.D. dissertation, Dept. Mech. Eng., Massachusetts Institute of Technology, Cambridge, MA, USA, 1988.
[12] D. Ogane, K. Hyodo, and H. Kobayashi, "Mechanism and control of a 7 DOF tendon-driven robotic arm with NST," *J. Robot. Soc. Jpn.*, vol. 14, no. 8, pp. 1152–1159, 1996, in Japanese.
[13] M. T. Mason and J. K. Salisbury, *Robot Hands and the Mechanics of Manipulation*. New York, NY, USA: MIT Press, 1985.
[14] S. C. Jacobsen, J. E. Wood, D. F. Knutti, and K. B. Biggers, "The UTAH/M.I.T. dexterous hand: Work in progress," *Int. J. Robot. Res.*, vol. 3, no. 4, pp. 21–50, 1984.
[15] S. Kawamura, H. Kino, and C. Won, "High-speed manipulation by using parallel wire-driven robots," *Robotica*, vol. 18, no. 1, pp. 18–21, 2000.
[16] I. Mizuuchi, T. Yoshikai, Y. Sodeyama, Y. Nakanishi, A. Miyadera, T. Yamamoto, T. Niemela, M. Hayashi, J. Urata, N. Y., T. Nishino, and M. Inaba, "Development of musculoskeletal humanoid Kotaro," in *Proc. IEEE Conf. Robot. Autom.*, May 2006, pp. 339–344.
[17] M. Kaneko, T. Yamashita, and K. Tanie, "Basic considerations on transmission characteristics for tendon drive robots," in *Proc. 5th Int. Conf. Adv. Robot.*, Jun. 1991, pp. 827–832.
[18] Y. J. Ou and L. W. Tsai, "Kinematic synthesis of tendon-driven manipulators with isotropic transmission characteristics," *Trans. ASME J. Mech. Design*, vol. 115, pp. 884–891, 1993.
[19] J. J. Lee and L. W. Tsai, "The structural synthesis of tendon-driven manipulators having a pseudotriangular structure matrix," *Int. J. Robot. Res.*, vol. 10, no. 3, pp. 255–262, 1991.
[20] H. Kobayashi, K. Hyodo, and D. Ogane, "On tendon-driven robotic mechanisms with redundant tendons," *Int. J. Robot. Res.*, vol. 17, no. 5, pp. 561–571, May 1998.
[21] H. Kobayashi and R. Ozawa, "Adaptive neural network control of tendon-driven mechanisms with elastic tendons," *Automatica*, vol. 39, no. 9, pp. 1509–1519, 2003.
[22] M. Grebenstein, M. Chalon, G. Hirzinger, and R. Siegwart, "Antagonistically driven finger design for the anthropomorphic DLR hand arm system," in *Proc. IEEE/RSJ Conf. Intell. Robots Syst.*, Taipei, Taiwan, Oct. 2010, pp. 609–616.
[23] S. K. Mustafa and S. K. Agrawal, "On the force-closure analysis of n-DOF cable-driven open chains based on reciprocal screw theory," *IEEE Trans. Robot.*, vol. 28, no. 1, pp. 22–31, Feb. 2012.
[24] D. E. Whitney, "Quasi-static assembly of compliantly supported rigid parts," *ASME J. Dyn. Syst., Meas., Control*, vol. 104, no. 1, pp. 65–67, 1982.
[25] H. Kobayashi, "On the articulated hands," in *The Robot. Research: The second International Symposium*. New York, NY, USA: MIT Press, 1985, pp. 293–300.
[26] Y. T. Lee, H. R. Choi, W. K. Chung, and Y. Youm, "Stiffness control of a coupled tendon-driven robot hand," *IEEE Control Syst. Mag.*, vol. 14, no. 5, pp. 10–19, Oct. 1994.
[27] A. Namiki, Y. Imai, M. Ishikawa, and M. Kankeko, "Development of a high-speed multifingered hand system and its application to catching," in *Proc. IEEE/RSJ Conf. Intell. Robots Syst.*, Las Vegas, NV, USA, Oct. 2003, pp. 2666–2671.
[28] N. Dechev, W. Cleghorn, and S. Naumann, "Multiple finger passive adaptive grasp prosthetic hand," *Mech. Mach. Theory*, vol. 36, pp. 1157–1173, 2001.
[29] W. Townsend, "The BarrettHand grasper—Programmably flexible part handling and assembly," *Ind. Robot*, vol. 27, no. 3, pp. 181–188, 2000.
[30] N. Fukaya, S. Toyama, T. Asfour, and R. Dillmann, "Design of the TUAT/Karlsruhe humanoid hand," in *Proc. IEEE/RSJ Conf. Intell. Robots Syst.*, 2000, pp. 1754–1759.
[31] H. Kawasaki, T. Komatsu, and K. Uchiyama, "Dexterous anthropomorphic robot hand with distributed tactile sensor: Gifu hand II," *IEEE/ASME Trans. Mechatronics*, vol. 7, no. 3, pp. 296–303, Sep. 2002.
[32] H. Liu, J. Butterfass, S. Knoch, P. Meusel, and G. Hirzinger, "A new control strategy for DLR's multisensory articulated hand," *IEEE Control Syst. Mag.*, vol. 19, no. 2, pp. 105–110, Apr. 1999.
[33] J. Pons, E. Rocon, R. Ceres, D. Reynaerts, B. Saro, S. Levin, and W. Van Moorleghem, "The MANUS-HAND dexterous robotics upper limb prosthesis: Mechanical and manipulation aspect," *Auton. Robots*, vol. 16, pp. 143–163, 2004.
[34] B. Massa, S. Roccella, M. C. Carrozza, and P. Dario, "Design and development of an underactuated prosthetic hand," in *Proc. IEEE Conf. Robot. Autom.*, Washington, DC, USA, May 2002, pp. 3374–3379.
[35] R. Cabas, L. M. Cabas, and C. Balaguer, "Optimized design of the underactuated robotic hand," in *Proc. IEEE Conf. Robot. Autom.*, Orlando, FL, USA, May 2006, pp. 982–987.
[36] S. Krut, "A force-isotropic underactuated finger," in *Proc. IEEE Conf. Robot. Autom.*, Barcelona, Spain, Apr. 2005, pp. 2314–2319.
[37] M. Higashimori, M. Kaneko, A. Namiki, and M. Ishikawa, "Design of the 100G capturing robot based on dynamic preshaping," *Int. J. Robot. Res.*, vol. 24, no. 9, pp. 743–553, 2005.
[38] F. Lotti, P. Tiezzi, G. Vassura, L. Biagiotti, G. Palli, and C. Melchiorri, "Development of UB hand 3: Early results," in *Proc. IEEE Conf. Robot. Autom.*, Barcelona, Spain, Apr. 2005, pp. 4488–4493.
[39] K. Kaneko, K. Harada, and F. Kanehiro, "Development of multi-fingered hand for life-size humanoid robots," in *Proc. IEEE Conf. Robot. Autom.*, Roma, Italy, Apr. 2007, pp. 913–920.
[40] H. Iwata and S. Sugano, "Design of anthropomorphic dexterous hand with passive joints and sensitive soft skins," in *Proc. SI Int.*, Tokyo, Japan, Dec. 2009, pp. 129–134.
[41] R. Ozawa, K. Hashirii, M. Moriya, and H. Kobayashi, "Design and control of a three-fingered tendon-driven robotic hand with active and passive tendons," *Auton. Robots*, Aug. 2013, DOI: 10.1007/s10514-013-9362-z.
[42] M. Catalano, G. Grioli, A. Serio, E. Farnioli, C. Pazza, and A. Bicchi, "Adaptive synergies for a humanoid robot hand," in *Proc. IEEE/RAS Conf. Humanoid Robots*, Osaka, Japan, Dec. 2012, pp. 7–14.
[43] J. L. Fu and N. S. Pollard, "On the importance of asymmetries in grasp quality metrics for tendon driven hands," in *Proc. IEEE/RSJ Conf. Intell. Robots Syst.*, Beijing, China, Oct. 2006, pp. 1068–1075.
[44] J. M. Inouye, J. J. Kutch, and F. J. Valero-Cuvas, "A novel synthesis of computational approaches enables optimization of grasp quality of tendon-driven hands," *IEEE Trans. Robot.*, vol. 28, no. 4, pp. 958–966, 2012.

Ryuta Ozawa (M'02) received the Ph.D. degree in mechanical engineering from Meiji University, Kawasaki, Japan, in 2001.

From 2001 to 2002, he was a Research Assistant at Meiji University. From 2002 to 2003 he was a Postdoctoral Research Fellow with the Japan Society for the Promotion of Science. He joined the Department of Robotics, Ritsumeikan University, Kyoto, Japan, in 2003. From 2008 to 2009, he was a Visiting Scholar with IRISA/INRIA, Rennes, France. He is currently an Associate Professor with the Department of Robotics, Ritsumeikan University. His research interests are manipulation of robotic hands and arms, teleoperation of robotic hands, full-actuated/underactuated tendon-driven robotic arms, mass estimation with a variable stiffness devises in micro gravity, balance control of a biped, and so on.

Dr. Ozawa received the Encouragement Prize for Young Researchers from the Department of System Integration, Society of Instrument and Control Engineers (SICE) of Japan, in 2006, the Best Paper Award from the Robotics Society of Japan in 2007, and the Outstanding Paper Prize from the Society of Instrument and Control Engineers of Japan in 2009. He is a member of the SICE, Japan Society of Mechanical Engineers, and the Robotics Society of Japan.

Hiroaki Kobayashi (M'89) received the B.E., M.E., and Ph.D. degrees in precision engineering in 1971, 1973, and 1977, respectively, all from Kyoto University, Kyoto, Japan.

Since 1976, he has been with the School of Science and Engineering, Meiji University, Kawasaki, Japan, where he is currently a Professor. From 1988 to 1989, he was a Postdoctoral Fellow in computer information science with the School of Engineering and Applied Science, University of Pennsylvania. His research interests are in the area of intelligent control of robotic systems, including machine learning.

Dr. Kobayashi is a member of Japan Society of Mechanical Engineers, SICE, the Institute of Systems, Control, and Information Engineers, and the Robotics Society of Japan.

Kazunori Hashirii was born in 1984. He received the B.S. and M.E. degrees in robotics and computer science from Ritsumeikan University, Kyoto, Japan, in 2007 and 2009, respectively.

He has worked for Nabel Co., Ltd, Japan, since 2009, and he is currently a Leader of the R&D Division of the Mechanical Design Group.